RSC Medicinal Chemistry

ROYAL SOCIETY OF CHEMISTRY

RESEARCH ARTICLE

Cite this: *RSC Med. Chem.*, 2022, **13**, 327

Design, synthesis and anti-mycobacterial evaluation of imidazo[1,2-*a*]pyridine analogues†

Yogesh Mahadu Khetmalis,[a] Surendar Chitti,[a] Anjani Umarani Wunnava,[b] Banoth Karan Kumar,[c] Muthyala Murali Krishna Kumar,[b] Sankaranarayanan Murugesan[c] and Kondapalli Venkata Gowri Chandra Sekhar *[a]

Based on the molecular hybridization strategy, thirty-four imidazo[1,2-*a*]pyridine amides (IPAs) and imidazo[1,2-*a*]pyridine sulfonamides (IPSs) were designed and synthesized. The structures of the target compounds were characterized using ^{1}H NMR, ^{13}C NMR, LCMS, and elemental analyses. The synthesized compounds were evaluated *in vitro* for anti-tubercular activity using the microplate Alamar Blue assay against *Mycobacterium tuberculosis* H37Rv strain and the MIC was determined. The evaluated compounds exhibited MIC in the range 0.05–≤100 μg mL^{-1}. Among these derivatives, **IPA-6** (MIC 0.05 μg mL^{-1}), **IPA-9** (MIC 0.4 μg mL^{-1}), and **IPS-1** (MIC 0.4 μg mL^{-1}) displayed excellent anti-TB activity, whereas compounds **IPA-5**, **IPA-7** and **IPS-16** showed good anti-TB activity (MIC 0.8–3.12 μg mL^{-1}). The most active compounds with MIC of <3.125 μg mL^{-1} were screened against human embryonic kidney cells to check their cytotoxicity to normal cells. It was observed that these compounds were nontoxic (SI value ≥66). The ADMET characteristics of the final compounds were also predicted *in silico*. Further, using the Glide module of Schrodinger software, a molecular docking study of **IPA-6** was carried out to estimate the binding pattern at the active site of enoyl acyl carrier protein reductase from *Mycobacterium tuberculosis* (PDB 4TZK). Finally, molecular dynamics simulations were performed for 100 ns to elucidate the stability, conformation, and intermolecular interactions of the co-crystal ligand and significantly active compound **IPA-6** on the selected target protein. **IPA-6**, the most active compound, was found to be 125 times more potent than the standard drug ethambutol (MIC 6.25 μg mL^{-1}).

Received 16th November 2021,
Accepted 3rd January 2022

DOI: 10.1039/d1md00367d

rsc.li/medchem

Introduction

Tuberculosis (TB) is regarded as one of the most ancient airborne infectious diseases known to humankind. TB is mainly caused by the bacillus *Mycobacterium tuberculosis* (MTB). It is the most common death-causing disease amongst patients with a single infectious agent. TB is primarily categorized as a pandemic, according to the World Health Organization (WHO). According to the WHO, there are approximately 1.35–1.52 million deaths concomitant with this infection every year. About 10 million people fall ill with TB *per annum*.[1] TB is of two types depending on the body organs it attacks; when it strikes the lungs, it is known as pulmonary TB, and when it affects other parts of the body, it is known as extra-pulmonary TB. Depending on the resistance to existing drugs, also two types, *viz.*, multi-drug-resistant (MDR-TB) and extensively drug-resistant tuberculosis (XDR-TB),[2,3] are known. TB is curable and treatable using a typical course of first-line anti-tubercular drugs such as isoniazid, rifampin, pyrazinamide, and ethambutol. Though second- and third-line drugs are also available for treating TB-resistant patients, they still have some significant disadvantages, such as long duration of treatment, higher cost involved for prolonged treatment, and poor drug compatibility.[4] Hence, the search for new anti-tubercular drugs with minimum side effects and better efficacy is still on.

Imidazo[1,2-*a*]pyridine (IPA) is one of the most prospective fused bicyclic heterocyclic rings that is accepted as a "drug preconception" scaffold due to its extensive range of applications in biology and pharmacology such as anticancer, antitubercular, antileishmanial, anticonvulsant, antimicrobial, antiviral, antidiabetic and proton pump

[a] *Department of Chemistry, Birla Institute of Technology and Science, Pilani, Hyderabad Campus, Jawahar Nagar, Hyderabad 500 078, Telangana, India. E-mail: kvgc@hyderabad.bits-pilani.ac.in, kvgcs.bits@gmail.com; Tel: +91 40 66303527*

[b] *College of Pharmaceutical Sciences, Andhra University, Visakhapatnam, Andhra Pradesh, 530 003, India*

[c] *Medicinal Chemistry Research Laboratory, Department of Pharmacy, Birla Institute of Technology and Science, Pilani, 333031, India*

† Electronic supplementary information (ESI) available. See DOI: 10.1039/d1md00367d

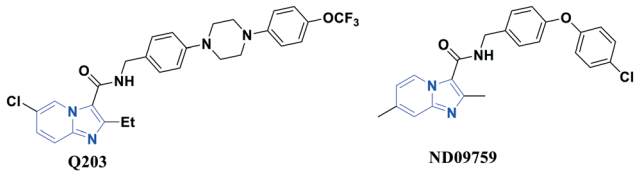

Fig. 1 Imidazo[1,2-*a*]pyridine-based anti-tubercular agents in clinical trials.

inhibitor activity.[5] Most of the imidazopyridine derivatives showed several potential therapeutic applications as drugs. Zolpidem was the first drug to enter the market and is used in the treatment of insomnia.[6] Alpidem (benzodiazepine receptor ligand), discovered in 1991, is used as an anxiolytic.[7,8] The drug olprinone is used as a cardiovascular agent.[9] Zolimidine, once used in the treatment of peptic ulcer and gastro-oesophageal reflux disease, is also based on the imidazopyridine skeleton.[10] Minodronic acid, a third-generation bisphosphonate drug, is used for the treatment of osteoporosis in Japan.[11]

Two derivatives, Q203 and ND09759, based on imidazo[1,2-*a*]pyridine, as anti-tubercular agents, are in clinical trials.[12,13] They were found to have excellent inhibitory effectiveness against drug-sensitive, MDR, and XDR strains for targeting MTB[14] (Fig. 1).

Many imidazo[1,2-*a*]pyridine (IPA) derivatives are reported to have anti-tubercular activity. Wu *et al.* in 2016 reported novel IPA derivatives containing the *N*-(2-phenoxyethyl) moiety as anti-tubercular agents. Among the compounds, **1** displayed a potent MIC value of 0.027 μg mL^{-1} against the drug-sensitive H37Rv strain isolated from MTB strains.[14] Gilish Jose *et al.* synthesized novel IPA derivatives and evaluated them for anti-TB activity. Among the compounds, **2** was the most active with MIC value of 6.25 μg mL^{-1} *in vitro* against MTB H37Rv.[15] Lokesh Pulipati and his group reported a series of twenty novel IPA carboxamides for anti-TB activity. Compound **3** was the most potent with MIC value of 0.78 μg mL^{-1} against MTB H37Rv strain.[16] Amongst the imidazo[1,2-*a*]pyridine compounds reported by Hongjian Wang *et al.*, **4** was the most active with MIC value of <0.035 μM against drug susceptible MTB H37Rv strain.[17] Apeng Wang *et al.* reported new anti-TB agents containing the imidazo[1,2-*a*]pyridine skeleton. Most of these displayed excellent inhibitory activity. Compound **5** was the best with MIC value of 0.0625 μg mL^{-1} against MTB strain H37Rv.[18] Compound **6** was the most potent amongst the IPA derivatives reported by Linhu Li *et al.* (MIC value <0.016 μg mL^{-1}).[19] Ganesh Samala and his group reported imidazo[1,2-*a*]pyridines as MTB pantothenate synthetase (PS) inhibitors. Compound **7** was determined to be the most active among all derivatives, with MIC of 4.53 μM against MTB PS.[20] Recently, imidazo[1,2-*a*]pyridine-3-carboxamide derivatives were reported by our group. Among all the compounds, **8** emerged to be the most potent with MIC of 13.74 μg mL^{-1}.[21] Literature-reported IPA-based anti-tubercular agents are showcased in Fig. 2.

Tetrahydropyridine scaffolds have recently been discovered in various natural and synthetic compounds with intriguing medicinal chemistry features. Tetrahydro-1*H*-pyrazolo-[4,3-*c*] pyridine derivatives were identified as novel MTB PS inhibitors by Samala *et al.* From this work, compound **9** was the most effective MTB PS inhibitor, with MIC value of 52.79 μM and MTB MIC of 26.7 μM.[22] Manvar's group synthesized novel dihydropyridine derivatives for anti-tubercular activity. Compound **10** was the most active with MIC value of >6.25 μg mL^{-1} against MTB H37Rv strain.[23] In medicinal chemistry, sulfonamide derivatives were found to have multifunctional and multitargeting properties. Recently, some research groups have reported sulfonamide derivatives as anti-tubercular agents. Konduri *et al.* reported piperazine derivatives with a sulfonyl functional group for anti-TB activity. Among all the compounds, analog **11** with MIC of 12.46 μM against MTB H37Rv strain was the most potent.[24] Raju and his group reported novel pyrazole sulfonamides as anti-TB agents. From this series, compound **12** with MIC of 6.25 μg mL^{-1} against MTB H37Rv strain was the

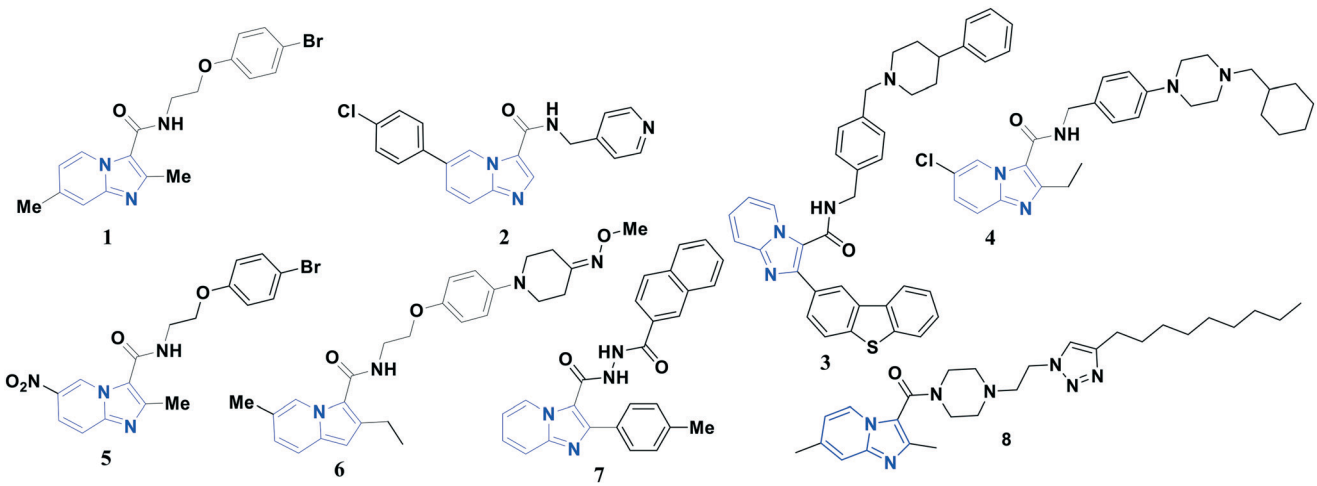

Fig. 2 Literature-reported imidazo[1,2-*a*]pyridine-based anti-tubercular agents.

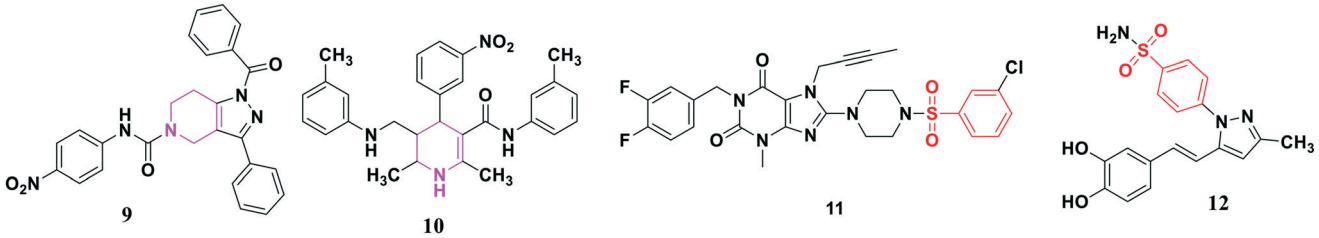

Fig. 3 Tetrahydropyridine- and sulfonamide-based anti-tubercular agents.

most active one.[25] Compounds exhibiting anti-tubercular activity based on the tetrahydropyridine and sulfonamide skeletons are depicted in Fig. 3.

The NADH/NADPH-dependent enoyl acyl carrier protein reductase (ENR/InhA) of MTB is one of the key enzymes that plays a significant role in the process of the fatty acid elongation cycle of MTB and mycolic acid biosynthesis. This is one of the validated effective molecular targets for discovering novel antimycobacterial agents.[26,27] It contains around 269 amino acid residues (single A chain) with one co-crystal ligand ((*R*)-1-cyclohexyl-*N*-(3,5-dichlorophenyl)-5-oxopyrrolidine-3-carboxamide) and one co-factor NAD in its 3D structure.[21] It also possesses a conserved active site and lacks apparent homologs in mammals.[28] A few reports mentioned above[21,26] also suggested the mode of action of antimycobacterial imidazopyridines through inhibition of InhA of MTB. Hence, based on the reported rationale, targeting the InhA enzyme followed by disruption of mycobacterial cellular homeostasis may be the most appropriate strategy for the current molecular docking study, and hence we docked our compounds at the active site of enoyl acyl carrier protein reductase from *Mycobacterium tuberculosis* (PDB 4TZK).

Molecular hybridization is one of the most acceptable ways for designing new pharmacological scaffolds as it encompasses multi-component reactions or pharmacophore units that are recognized and generated from known biological units. In recognition of the significance of imidazopyridines, 1,2,3,6-tetrahydropyridines and sulfonamides as anti-tubercular agents, in the current work, these scaffolds were hybridized into a single framework and novel anti-tubercular agents **IPA 1–17** and **IPS 1–17** were designed and synthesized (Fig. 4).

Results and discussion

Chemistry

In this research, analogues of 1-(4-(2-(3,4-dimethoxy phenyl)-imidazo[1,2-*a*]pyridin-6-yl)-5,6-dihydropyridin-1(2*H*)-yl) amide (**IPA 1–17**) and 2-(3,4-dimethoxyphenyl)-6-(1-(sulfonyl)-1,2,3,6-tetrahydropyridin-4-yl)-imidazo[1,2-*a*]pyridine (**IPS 1–17**) are synthesized as depicted in Schemes 1 and 2. The experimental methodologies are described in full in the ESI† as well as in a recently published article by our group.[11]

Thin layer chromatography (TLC) and ESI mass spectrometry (ESI-MS) were used to monitor the reactions in each step. Every step's crude products were purified using column chromatography with silica gel (100–200 mesh size) and EtOAc in hexane as the eluent (10–100%). ESI-MS, ^{1}H NMR, ^{13}C NMR, and elemental analyses were used to confirm

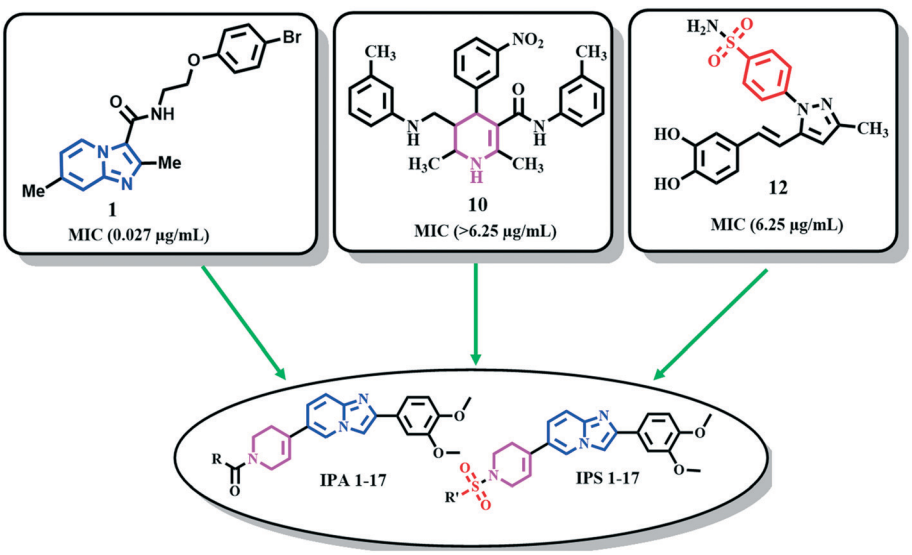

Fig. 4 Scaffold design strategy for new anti-tubercular agents.

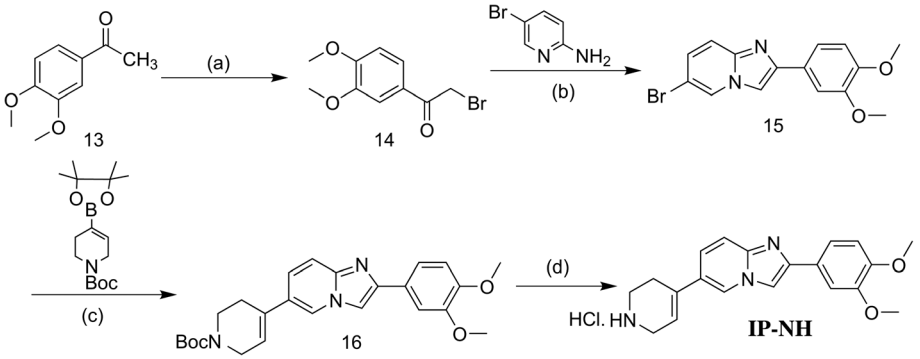

Scheme 1 Reaction conditions: (a) tetrabutylammonium tribromide (TBATB), MeOH–CH_2Cl_2, rt, 16 h, (b) 2-amino-5-bromo pyridine, ethanol, 70 °C, 16 h, (c) 2 M Na_2CO_3, Pd(dppf)Cl_2, 1,4-dioxane, 90 °C, 16 h, (d) Me_3SiCl, 2,2,2-trifluoroethanol, 0 °C–rt, 2 h.

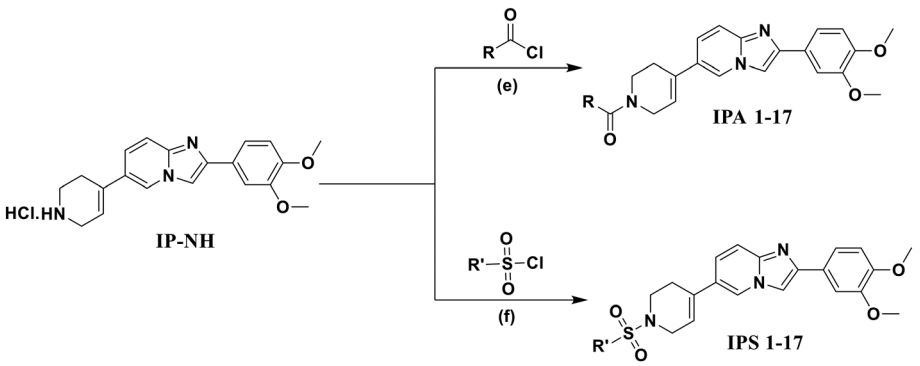

Scheme 2 Reaction conditions: (e) various acid chlorides, *N*,*N*-diisopropylethylamine (Hunig's base), CH_2Cl_2, 0 °C–rt, 2 h, (f) various sulfonyl chlorides, Hunig's base, CH_2Cl_2, 0 °C–rt, 2 h.

all the synthesized compounds. The capability of the synthesized imidazo[1,2-*a*]pyridine amide (IPA) and imidazo[1,2-*a*]pyridine sulfonamide (IPS) derivatives to exhibit anti-mycobacterial activity was assessed. The majority of the IPA series compounds showed excellent anti-TB activity, while some IPS series compounds were very good.

In vitro anti-mycobacterial evaluation of the final compounds

The anti-mycobacterial activity of the title compounds was tested *in vitro* against MTB H37Rv strain using the MABA method.[29,30] The activity results are shown in Table 1. The assay for the compounds with codes **IPA-6**, **IPA-9** and **IPS-1** showed anti-mycobacterial activity better than that of the standard (ethambutol and *p*-aminosalicylic acid) and MABA assay was carried out with further dilutions to ascertain the MIC of those compounds. The MIC for **IPA-6** was 0.05 μg mL^{-1} and for **IPA-9** and **IPS-1** was 0.4 μg mL^{-1}.

Cytotoxicity studies

The most promising compounds, **IPA-4**, **IPA-6**, **IPA-7**, **IPA-9**, and **IPS-1**, with MIC of <3.125 μg mL^{-1}, were tested against human embryonic kidney (HEK) cells to see if they were toxic to normal cells. These compounds' IC_{50} values were evaluated in ten different dosages (1.0 mM–1.9 μM) on HEK-293 cells for 48 hours, and cell viability was measured using the MTT assay.[11] It was observed that all these compounds were nontoxic to normal human cells.[11] They exhibited selectivity index (SI) values of ≥66. The IC_{50} values and SI values are tabulated in Table 2.

Structure–activity relationship (SAR) studies

Among the synthesized IPA derivatives, compounds containing an aryl group attached to the carbonyl carbon of the amide (–Ph and substituted phenyl) exerted remarkable antitubercular activity. Amongst these, **IPA-6** with MIC of 0.05 μg mL^{-1} was found to be the most active compound and is 125 times more potent than the standard drug ethambutol (MIC 6.25 μg mL^{-1}). The presence of electron-withdrawing –Cl at the *para* position of the phenyl (**IPA-9**) resulted in a 16 times more potent compound (MIC 0.4 μg mL^{-1}) than ethambutol. **IPA-5**, a *p*-toluyl substituted compound, exhibited good anti-TB activity with MIC 0.8 μg mL^{-1}, while introduction of a cyclic group (**IPA-7**, cyclobutyl) yielded a compound with MIC of 1.56 μg mL^{-1}. Heterocyclic amides (**IPA-13–17**) showed substantially lower potency with MIC of ≥50 μg mL^{-1}. In the case of IPS series compounds, those with aliphatic methyl substitution (–CH_3) moieties linked to the sulfonyl group (**IPS-1**) showed remarkable anti-TB activity with MIC of 0.4 μg mL^{-1}. Compounds having a halogen atom (–Br) and an aryl functional group in the IPS class showed

Table 1 Anti-mycobacterial activity of the title compounds

S. no	Entry	R/R′	MIC (μg mL^{-1})
1	**IPA-1**	CH_3	>100
2	**IPA-2**	$C(CH_3)_3$	100
3	**IPA-3**	Cyclopropyl	50
4	**IPA-4**	Cyclobutyl	1.56
5	**IPA-5**	Cyclohexyl	50
6	**IPA-6**	C_6H_5	0.05
7	**IPA-7**	4-$CH_3C_6H_4$	0.8
8	**IPA-8**	4-FC_6H_4	25
9	**IPA-9**	4-ClC_6H_4	0.4
10	**IPA-10**	2-FC_6H_4	6.25
11	**IPA-11**	3-FC_6H_4	50
12	**IPA-12**	3-$CF_3C_6H_4$	12.5
13	**IPA-13**	2-Pyridyl	100
14	**IPA-14**	2-Thiophenyl	25
15	**IPA-15**	2-Furanyl	50
16	**IPA-16**	4-Oxazolyl	50
17	**IPA-17**	2-Benzyloxy	50
18	**IPS-1**	CH_3	0.4
19	**IPS-2**	CH_3CH_2	12.5
20	**IPS-3**	$CH_3(CH_2)_2$	12.5
21	**IPS-4**	Cyclopropyl	12.5
22	**IPS-5**	Cyclopentyl	25
23	**IPS-6**	Cyclohexyl	25
24	**IPS-7**	C_6H_5	25
25	**IPS-8**	4-$CH_3C_6H_4$	25
26	**IPS-9**	4-FC_6H_4	6.25
27	**IPS-10**	4-ClC_6H_4	6.25
28	**IPS-11**	4-$C(CH_3)_3C_6H_4$	6.25
29	**IPS-12**	4-$CH_3COC_6H_3$	6.25
30	**IPS-13**	4-BrC_6H_4	6.25
31	**IPS-14**	4-$NO_2C_6H_4$	6.25
32	**IPS-15**	5-Cl-thiophenyl	6.25
33	**IPS-16**	5-Br-thiophenyl	3.125
34	**IPS-17**	4-$CF_3C_6H_4$	6.25
35	*p*-Aminosalicylic acid	—	12.5
36	Ethambutol	—	6.25

Table 2 IC_{50} and selectivity index values of selected active compounds

Entry	MIC (μg mL^{-1}) in MTB H37Rv	IC_{50} (HEK cells)	SI value
IPA-4	1.56	102.88 ± 2.06	66
IPA-6	0.05	72.1 ± 2.52	1442
IPA-7	0.8	84.06 ± 1.72	106
IPA-9	0.4	75.99 ± 2.49	190
IPS-1	0.4	101.34 ± 2.31	253

good anti-TB activity (**IPS-16**) with MIC of 3.125 μg mL^{-1}. The rest of the compounds with *ortho* substitutions and electron-withdrawing groups on the phenyl ring exhibited moderate to weak anti-TB activity. The structural and anti-TB activity SAR investigations revealed that the imidazo[1,2-*a*]pyridine amide (IPA) analogues were more active than the imidazo[1,2-*a*]pyridine sulfonamide (IPS) derivatives. A summary of the SAR is depicted in Fig. 5.

Summary of the SAR of the IPA and IPS series compounds

***In silico* predicted ADMET studies.** Any new chemical molecule must meet the physicochemical parameters established by Lipinski's rule of five in order to be absorbed orally. Through *in silico* approaches, it is possible to predict the same parameters that will be established when a new candidate molecule is found. As can be seen in Table 3, the *in silico* results for the thirty-four final analogues were deduced. As a rule of five, Lipinski's law fitted the forecast parameters of analogues within their prescribed ranges for all the parameters, including molecular weights, hydrogen bond acceptors, hydrogen bond donors and violation of rules except partition coefficients. Except for aqueous solubility, most compounds in the current study followed the Jorgensen rule of three. Concerning the predicted results of the title analogues, it appears likely that these compounds will not encounter any pharmacokinetic challenges during the development phase of drug discovery.

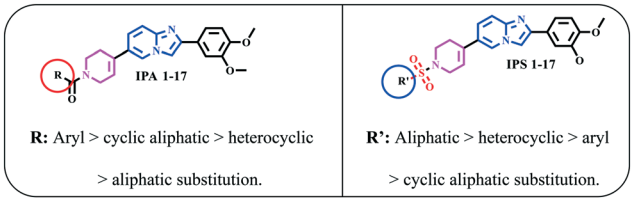

Fig. 5 Summary of the SAR of the IPA and IPS series compounds.

Molecular docking studies

The MTB (strain ATCC 25618/H37Rv) enoyl acyl carrier protein reductase (ENR) crystal structure (PDB 4TZK)[31] with a resolution of 1.62 Å has been retrieved from the Protein Data Bank.[32] As a validated, important target for antimycobacterial agents, the ENR of MTB is also one of the critical enzymes involved in the elongation of fatty acids in mycobacteria. The single A chain with 269 sequence length residues has one co-crystal ligand ((*R*)-1-cyclohexyl-*N*-(3,5-dichlorophenyl)-5-oxopyrrolidine-3-carboxamide) and one co-factor NAD linked to it.

Validation of the docking protocol

As a pre-selection step for testing the docking protocols for the final compounds, we followed the protocols already established in our previous studies.[21,33] In accordance with Fig. 6, the RMSD for the target protein was 0.4 Å, signifying that the docking protocol was both reliable and ready for subsequent comparative studies (Table 4). The figures show detailed visualization of an interactive 3D and 2D diagram of the co-crystal ligand (Fig. 7) and the most active compound **IPA-6** (Fig. 8) in the active site of the target protein.

A binding conformation appears to be possible with compound **IPA-6** based on *in silico* docking studies. The co-crystallized ligand exhibited an outstanding docking score of −11.08 kcal mol^{-1}. Based on close examinations of the 2D and 3D representation of co-crystallized ligand (Fig. 7), the amino acid residue TYR-158 (distance 1.99 Å) of protein was discovered to form a hydrogen bond. In addition to hydrogen bonding, the co-crystal ligand formed aromatic bonding interactions with PRO-156 (distance 2.57 Å) and halogen

Table 3 *In silico* predicted physicochemical parameters of the title compounds

	Lipinski rule of five					Jorgensen rule of three			
Codes	mol MW	Donor HB	accept HB	log Po/w	No. of violations of rule of five	log *S*	PCaco	metab	No. of violations of rule of three
IPA-1	377.44	0	6	3.61	0	−4.91	1362.24	4	0
IPA-2	419.52	0	6	4.66	0	−6.17	2356.21	4	1
IPA-3	403.48	0	6	4.30	0	−6.00	2387.67	4	1
IPA-4	417.51	0	6	4.56	0	−6.22	2465.12	5	1
IPA-5	445.56	0	6	5.19	1	−7.10	2411.94	5	1
IPA-6	439.51	0	6	5.62	1	−7.45	3022.04	4	1
IPA-7	453.54	0	6	5.95	1	−8.06	3021.67	5	1
IPA-8	457.50	0	6	5.80	1	−7.66	3020.45	4	1
IPA-9	473.96	0	6	6.13	1	−8.22	3015.25	4	1
IPA-10	457.50	0	6	5.79	1	−7.57	3071.45	4	1
IPA-11	457.50	0	6	5.86	1	−7.83	3013.02	4	1
IPA-12	507.51	0	6	6.58	2	−8.77	2841.94	5	1
IPA-13	440.50	0	7	4.86	0	−6.82	1781.79	5	1
IPA-14	445.54	0	6	5.51	1	−7.35	2999.02	5	1
IPA-15	429.47	0	6.5	4.95	0	−6.68	2785.28	5	1
IPA-16	430.46	0	8	3.88	0	−5.40	2179.13	5	0
IPA-17	483.57	0	7.7	5.25	1	−6.97	1862.59	7	2
IPS-1	413.49	0	7.5	3.61	0	−5.37	1546.98	4	0
IPS-2	427.52	0	7.5	4.06	0	−5.76	1981.46	4	1
IPS-3	441.54	0	7.5	4.45	0	−6.21	1981.68	4	1
IPS-4	439.53	0	7.5	4.25	0	−6.01	2002.68	4	1
IPS-5	467.58	0	7.5	4.85	0	−6.68	2364.89	4	1
IPS-6	481.61	0	7.5	5.18	1	−7.13	2412.48	4	1
IPS-7	475.56	0	7.5	5.14	1	−7.47	1274.58	4	1
IPS-8	489.59	0	7.5	5.33	1	−7.37	2031.46	5	1
IPS-9	493.55	0	7.5	5.23	1	−7.11	2030.95	4	1
IPS-10	510.01	0	7.5	5.50	2	−7.51	2027.93	4	1
IPS-11	531.67	0	7.5	6.29	2	−8.48	2038.51	4	1
IPS-12	517.60	0	9.5	4.34	1	−6.77	594.53	4	1
IPS-13	554.46	0	7.5	5.58	2	−7.63	2026.81	4	1
IPS-14	520.56	0	8.5	4.24	1	−6.78	243.24	5	1
IPS-15	516.03	0	7.5	5.42	2	−7.51	1897.72	5	1
IPS-16	560.48	0	7.5	5.50	2	−7.64	1897.45	5	1
IPS-17	543.56	0	7.5	6.01	2	−8.25	2032.36	4	1

Description: Lipinski's rule of five – number of violations of Lipinski's rule of five. The rules are mol MW 130.0–725.0, log Po/w 2.0–6.5, donor HB ≤5, accept HB ≤10 and maximum 4 violations. Description: Jorgensen's rule of three – number of violations of Jorgensen's rule of three. The three rules are log *S* −6.5–0.5, PCaco <25 poor, >500 great, primary metabolites <7. Compounds with fewer (and preferably no) violations of these rules are more likely to be orally available (values reported in QikProp).

bonding interactions with GLY-104 (distance 3.02 Å). These interactions increased the stability of the co-crystallized ligand in the active site of the target protein, resulting in a significant docking score.

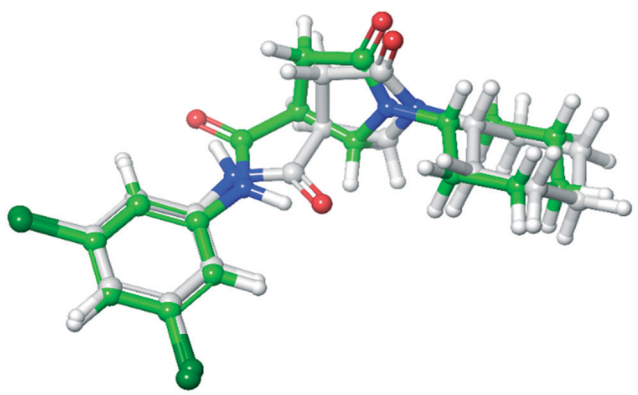

Fig. 6 Overlap position of re-docked pose of co-crystal ligand (white) with its X-ray pose (green) in the active site of the target (PDB 4TZK).

It was observed that the same amino acid, TYR-158, was found to be involved in the hydrogen bond contact with compound **IPA-6** (distance 2.15 Å). Furthermore, it was involved in pi-stacking with the phenyl ring (distance 4.64 Å). Surprisingly, a new amino acid, GLN-100, was also discovered in the same hydrogen bond interaction with the methoxy oxygen at 2.31 Å. Based on these strong binding patterns, compound **IPA-6** was found to have significant anti-mycobacterial potency with MIC of 0.05 μg mL^{-1}.

Molecular dynamics (MD) studies

MD simulations were performed to elucidate the stability, conformation and intermolecular interactions of the ligand molecules on the enoyl acyl carrier protein reductase (ENR) target. The Desmond package (academic version 2020) was used to calculate time-dependent dynamic changes of docked complexes. Simulations using SPC were carried out at 310.15 K and 1.2 bar pressure. Over a 100 ns MD simulation, Fig. 9 depicts the root-mean-square deviation (RMSD) plot of the

Table 4 Amino acid interactions and docking scores exhibited by the co-crystal ligand and compound **IPA-6**

	Amino acid involved in the interactions	Type of bond	Distance (Å)	Glide score (kcal/mol)
Co-crystal ligand	TYR-158	Hydrogen bond	1.99	−11.08
	PRO-156	Aromatic bond	2.57	
	GLY-104	Halogen bond	3.02	
IPA-6	TYR-158	Hydrogen bond	2.15	−7.27
	TYR-158	Pi–pi bond	4.64	
	GLN-100	Hydrogen bond	2.31	

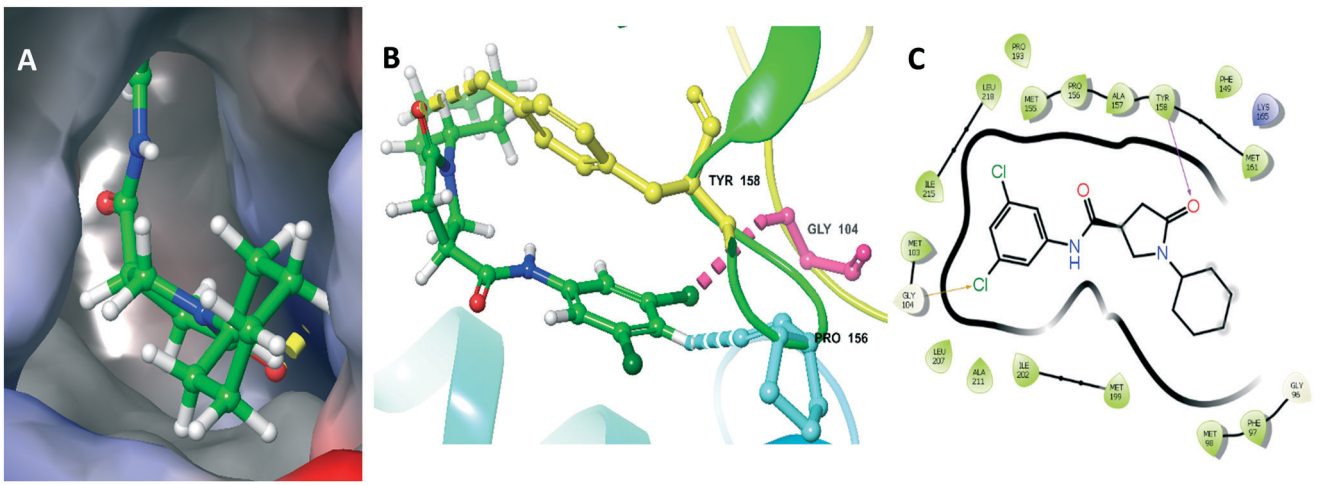

Fig. 7 Interactive diagram of the co-crystal ligand in the active site of the target PDB 4TZK. (A) Electrostatic surface of the co-crystal ligand. (B) 3D image. (C) 2D image. Color interpretation: blue, aromatic bond; yellow, hydrogen bond; and magenta, halogen bond in 3D interaction. Magenta, hydrogen bond and yellow, halogen bond in 2D interaction.

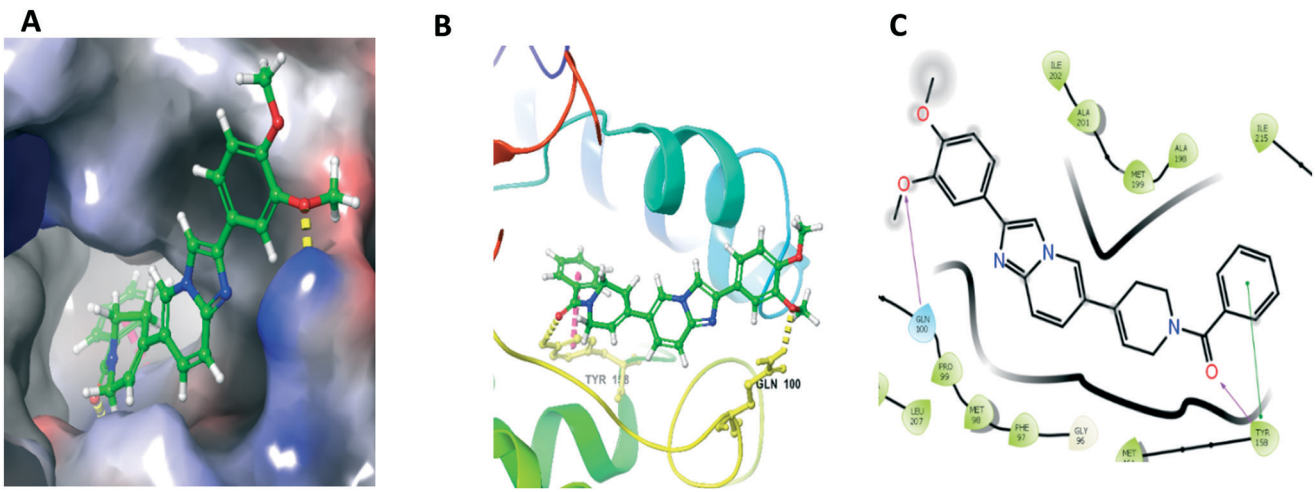

Fig. 8 Interactive diagram of compound **IPA-6** in the active site of the target PDB 4TZK. (A) Electrostatic surface of the co-crystal ligand. (B) 3D image. (C) 2D image. Color interpretation: blue, aromatic bond; yellow, hydrogen bond; and magenta, halogen bond in 3D interaction. Magenta, hydrogen bond and green, pi interaction in 2D interaction.

co-crystal ligand and significantly active compound **IPA-6**. According to MD simulations, docked complexes of the co-crystal ligand and substantially active compound **IPA-6** (protein–ligand complex or PLC) align with the enoyl acyl carrier protein reductase target. The RMSD of the PLC was 3–5 Å, which indicates its extraordinarily high stability under simulated conditions based on standard reports for small biomolecular complexes. At around 30–35 ns of simulation with 3.6 Å fluctuation, the co-crystal ligand went into the groove of the target and it oscillated. After a slight variation, the PLC turned into a most stable complex throughout the 100 ns simulation. The significantly active compound **IPA-6**

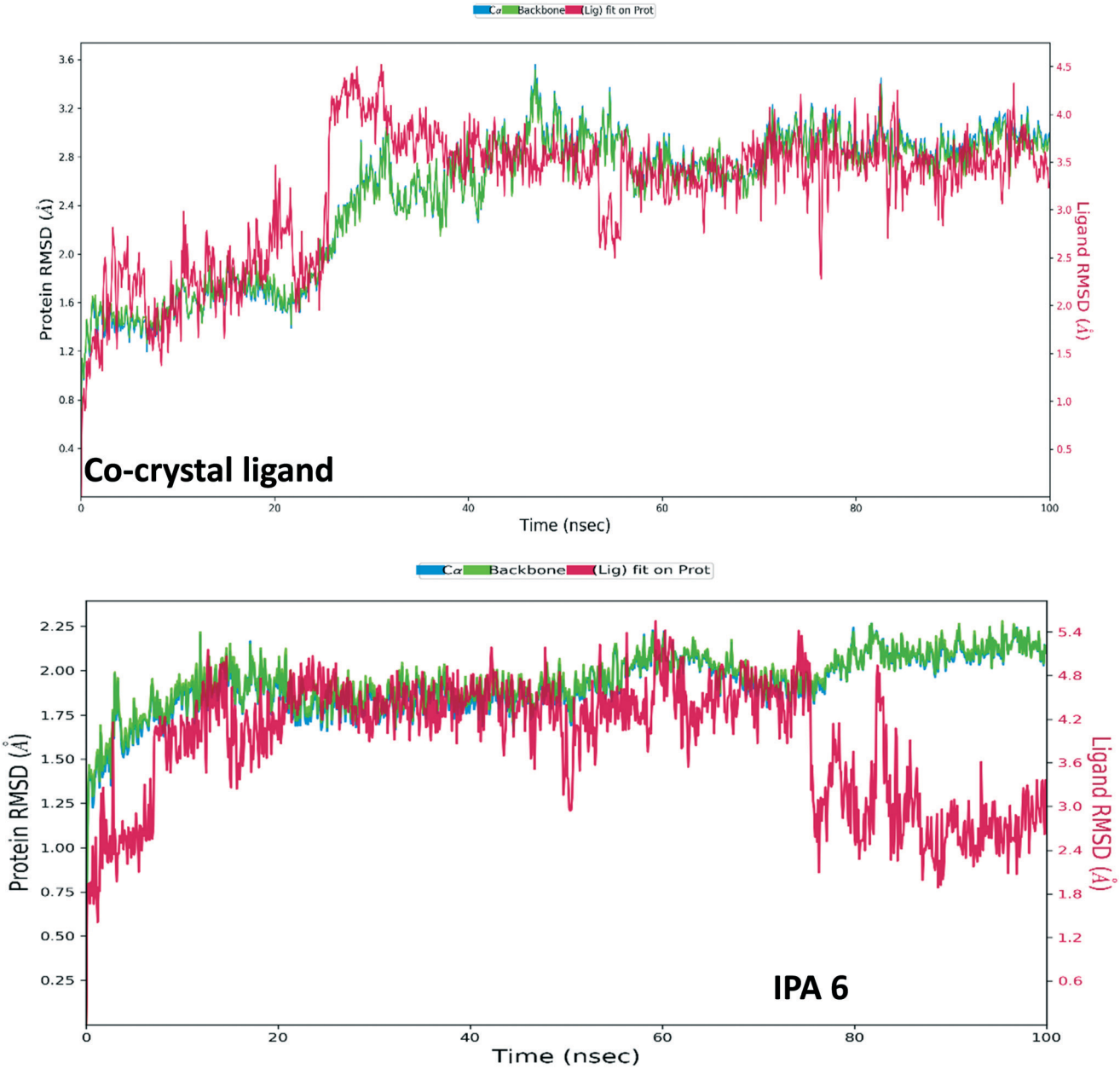

Fig. 9 Root-mean-square deviation of the co-crystal ligand and **IPA-6** in its active site.

showed strong interaction in the active site up to 78 ns. Compound **IPA-6** exhibited an unstable condition after 78 ns of the simulation period. All frames from the MD simulation were critically observed. It was observed that, apart from the keto group in the compound **IPA-6**, the remaining portions, of the compound, were protruding towards the solvent accessible surface area. As a result, the compound **IPA-6** MD is more fluctuated towards the end stage.

During simulations of both the co-crystal ligand and compound **IPA-6**, it was observed that TYR-158 produced an active hydrogen bond with both PLCs. Apart from that, amino acid residue ALA-198 in the co-crystal ligand and GLN 100 in compound **IPA-6** also revealed hydrogen bond interactions, as shown in Fig. 9. Amino acid residue ALA-198 actively contributed 65% with the amide NH in the co-crystal ligand, whereas in the case of compound **IPA-6**, the keto group revealed 75% of hydrogen bonds with TYR-158 amino acid residue (Fig. 10). Apart from hydrogen bonds, water-mediated interactions were also commonly observed in both the PLCs. Fig. 11 depicts the percentage of amino acid interactions during MD simulation of the co-crystal ligand and compound **IPA-6**.

Conclusion

In conclusion, we have designed and synthesized thirty-four novel imidazo[1,2-*a*]pyridine amide (IPA) and imidazo[1,2-*a*]

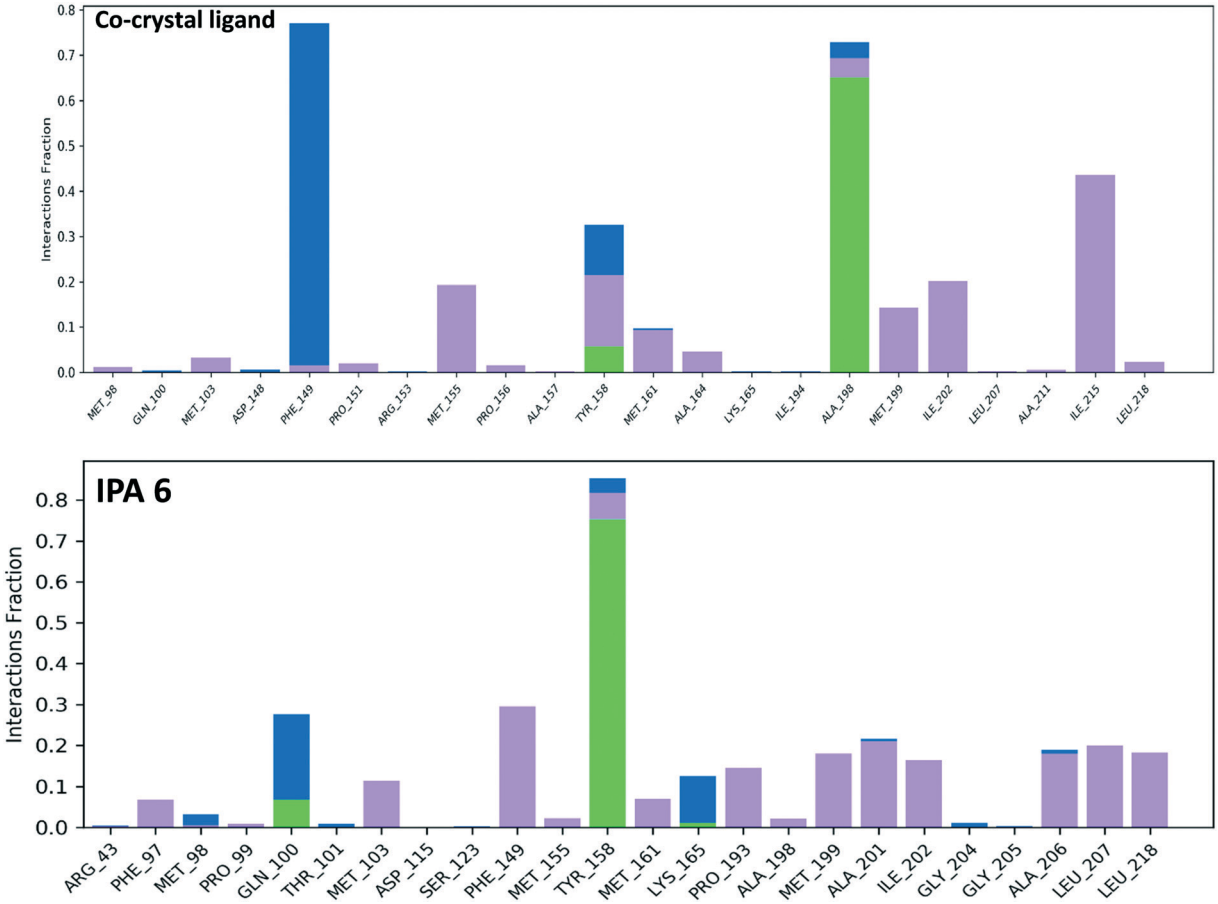

Fig. 10 Vital amino acid interactions during MD simulation of the co-crystal ligand and **IPA-6**.

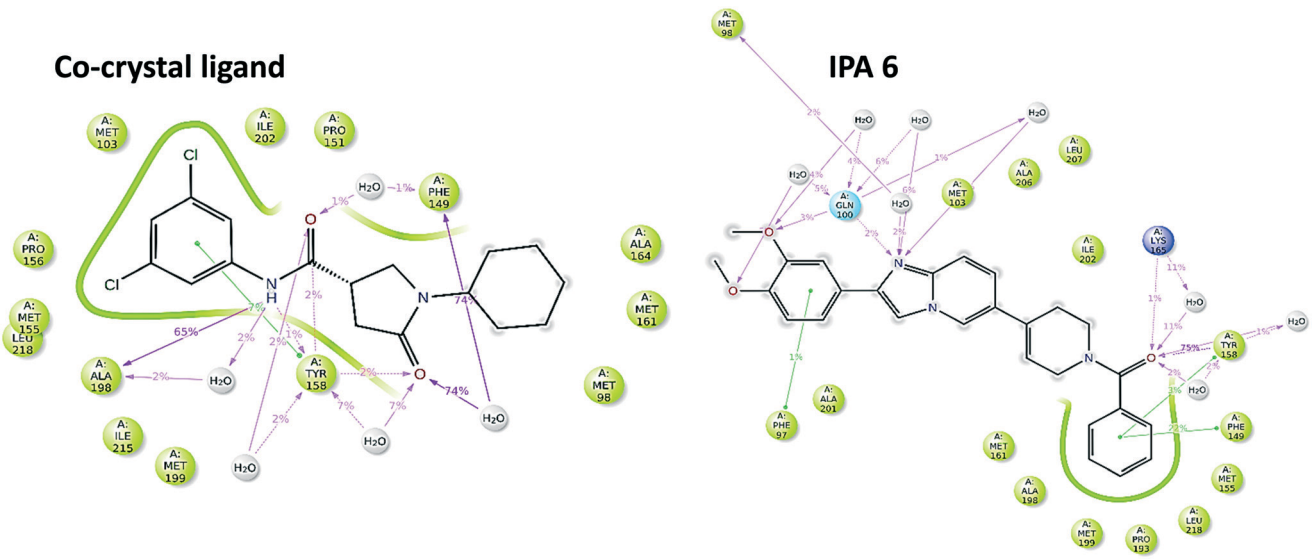

Fig. 11 Percentage of amino acid interactions during MD simulation of the co-crystal ligand and compound **IPA-6**.

pyridine sulfonamide (IPS) derivatives and screened them for *in vitro* anti-TB activity against MTB H37Rv strain. The synthesized derivatives were confirmed using ^{1}H NMR, ^{13}C NMR, ESI mass spectrometry, and elemental analyses. The compounds exhibited excellent to moderate anti-tubercular activity against the tested strains. Compounds **IPA-6** (MIC 0.05 μg mL^{-1}), **IPA-9** (MIC 0.4 μg mL^{-1}) and **IPS-1** (MIC 0.4 μg mL^{-1}) displayed excellent anti-TB activity, whereas compounds **IPA-5**, **IPA-7** and **IPS-16** (MIC 0.8–3.12 μg mL^{-1}) showed moderate to good anti-TB activity in the MABA

method. It was observed that all these compounds were nontoxic to normal human cells as against human embryonic kidney (HEK) cells. The five best compounds exhibited a SI value of ≥66. Furthermore, *in silico* ADMET values predicted for the title compounds were found to be within the range of the marketed drugs. The most active compound **IPA-6**, docked with enoyl acyl carrier protein reductase (PDB 4TZK), revealed a hydrogen bond contact with the surrounding amino acid residue TYR-158 (distance 1.99 Å) as well as an aromatic bond connection with PRO-156 (distance 2.57 Å). Finally, MD simulations were performed for 100 ns to elucidate the stability, conformation and intermolecular interactions of the co-crystal ligand and significantly active compound **IPA-6** on the target enoyl acyl carrier protein reductase (ENR). **IPA-6**, the most active compound from this work, was found to be 125 times more potent than the standard drug ethambutol (MIC 6.25 μg mL^{-1}).

Experimental section

In the ESI,† the general procedure for synthesized intermediates and final products is described in detail. Procedures related to biology experiments, *viz*., anti-TB MABA assay, cytotoxicity studies and docking studies, are outlined in the ESI.†

Analytical data for the final compounds (IPA 1–17) and (IPS 1–17)

1-(4-(2-(3,4-Dimethoxyphenyl)-imidazo[1,2-*a*]pyridin-6-yl)-5,6-dihydropyridin-1(2*H*)-yl)-ethanone (IPA-1). Off-white solid; m.p. 146–148 °C; yield 94%, 0.240 g, ^{1}H NMR (400 MHz, MeOH-d_4): δ 8.34 (d, J = 3.2 Hz, 1H), 8.00 (s, 1H), 7.52 (d, J = 9.2 Hz, 1H), 7.43 (d, J = 9.2 Hz, 1H), 7.38 (s, 1H), 7.32 (d, J = 8.0 Hz, 1H), 6.92 (d, J = 8.4 Hz, 1H), 6.18 (s, 1H), 4.14 (d, J = 2.8 Hz, 2H), 3.82 (s, 3H), 3.77 (s, 3H), 3.72 (t, J = 5.6 Hz, 1H), 3.67 (t, J = 5.6 Hz, 1H), 2.54 (s, 1H), 2.45 (s, 1H), 2.07 (d, J = 15.2 Hz, 3H). ^{13}C NMR (101 MHz, DMSO-d_6): δ 154.98, 154.64, 149.16, 145.41, 144.41, 131.92, 127.13, 124.53, 123.09, 120.11, 119.77, 118.47, 116.48, 115.37, 112.49, 109.65, 56.01, 55.95, 44.82, 43.63, 27.02, 25.75. ESI MS (*m*/*z*): calcd for $C_{22}H_{23}N_3O_3$, 377.44; found 378.1 $[M + H]^+$. Anal. calcd for $C_{22}H_{23}N_3O_3$ (%): C, 70.01; H, 6.14; N, 11.13; O, 12.72; found: C, 70.05; H, 6.12; N, 11.18; O, 12.70.

1-(4-(2-(3,4-Dimethoxyphenyl)-imidazo[1,2-*a*]pyridin-6-yl)-5,6-dihydropyridin-1(2*H*)-yl)-2,2-dimethylpropan-1-one (IPA-2). Off-white solid; m.p. 97–99 °C; yield 78%, 0.220 g; ^{1}H NMR (400 MHz, DMSO-d_6): δ 8.23 (s, 1H), 7.91 (s, 1H), 7.40–7.30 (m, 4H), 6.88 (d, J = 8.4 Hz, 1H), 6.13 (s, 1H), 4.17 (s, 2H), 3.81 (s, 3H), 3.78 (d, J = 5.6 Hz, 2H), 3.75 (s, 3H), 2.46 (s, 2H), 1.22 (s, 9H). ^{13}C NMR (101 MHz, DMSO-d_6): δ 167.92, 159.69, 154.79, 149.65, 147.52, 135.94, 131.42, 129.58, 127.48, 124.78, 121.63, 120.41, 118.57, 117.64, 115.47, 113.46, 61.79, 58.97, 49.52, 46.73, 39.42, 28.37. ESI MS (*m*/*z*): calcd for $C_{25}H_{29}N_3O_3$, 419.52, found 420.19 $[M + H]^+$. Anal. calcd for $C_{25}H_{29}N_3O_3$ (%): C, 71.57; H, 6.97; N, 10.02; O, 11.44; found: C, 71.50; H, 6.91; N, 10.00; O, 11.10.

Cyclopropyl-(4-(2-(3,4-dimethoxyphenyl)-imidazo[1,2-*a*]pyridin-6-yl)-5,6-dihydropyridin-1(2*H*)-yl)methanone (IPA-3). Off-white solid; m.p. 157–159 °C; yield 75%, 0.205 g; ^{1}H NMR (400 MHz, MeOH-d_4): δ 8.31 (s, 1H), 7.97 (s, 1H), 7.42–7.33 (m, 4H), 6.91 (d, J = 8.4 Hz, 1H), 6.17 (d, J = 9.2 Hz, 1H), 4.37 (s, 1H), 4.14 (s, 1H), 3.90 (t, J = 5.6 Hz, 1H), 3.82 (s, 3H), 3.77 (s, 3H), 3.74 (t, J = 5.6 Hz, 1H), 2.57 (s, 1H), 2.45 (s, 1H), 1.97–1.86 (dd, J = 4.0, 4.4 Hz 1H), 0.82–0.79 (m, 2H), 0.77–0.74 (m, 2H). ^{13}C NMR (101 MHz, DMSO-d_6): δ 159.26, 157.62, 151.36, 147.41, 145.41, 132.92, 129.54, 126.73, 124.09, 121.72, 119.86, 118.53, 117.48, 116.37, 113.49, 111.65, 57.29, 56.95, 45.32, 44.63, 29.52, 26.73, 15.73, 8.42. ESI MS (*m*/*z*): calcd for $C_{24}H_{25}N_3O_3$, 403.47; found 404.1 $[M + H]^+$. Anal. calcd for $C_{24}H_{25}N_3O_3$ (%): C, 71.44; H, 6.25; N, 10.41; O, 11.90; found: C, 71.40; H, 6.30; N, 15.41; O, 11.12.

Cyclobutyl-(4-(2-(3,4-dimethoxyphenyl)-imidazo[1,2-*a*]pyridin-6-yl)-5,6-dihydropyridin-1(2*H*)-yl)-methanone (IPA-4). Off-white solid; m.p. 163–165 °C; yield 70%, 0.196 g; ^{1}H NMR (400 MHz, MeOH-d_4): δ 8.31 (d, J = 6.8 Hz 1H), 7.98 (s, 1H), 7.43–7.34 (m, 4H), 6.92 (d, J = 8.4 Hz, 1H), 6.15 (d, J = 15.2 Hz, 1H), 4.12 (d, J = 2.4 Hz 1H), 4.0 (d, J = 2.4 Hz 1H), 3.83 (s, 3H), 3.77 (s, 3H), 3.73 (t, J = 5.6 Hz, 1H), 3.57 (t, J = 5.6 Hz, 1H), 3.46–3.31 (m, 2H), 2.47 (d, J = 13.6 Hz, 1H), 2.26–2.11 (m, 4H), 1.98–1.94 (m, 1H), 1.91–1.81 (m, 1H). ^{13}C NMR (101 MHz, DMSO-d_6): δ 161.26, 159.67, 154.34, 149.57, 147.63, 134.97, 130.54, 128.46, 126.37, 123.76, 121.86, 119.53, 118.42, 116.92, 114.73, 112.65, 58.72, 57.95, 47.32, 45.63, 30.52, 27.53, 16.74. ESI MS (*m*/*z*): calcd for $C_{25}H_{27}N_3O_3$, 417.5; found 418.1 $[M + H]^+$. Anal. calcd for $C_{25}H_{27}N_3O_3$ (%): C, 71.92; H, 6.52; N, 10.06; O, 11.50; found: C, 71.90; H, 6.55; N, 10.10; O, 11.45.

Cyclohexyl-(4-(2-(3,4-dimethoxyphenyl)-imidazo[1,2-*a*]pyridin-6-yl)-5,6-dihydropyridin-1(2*H*)-yl)-methanone (IPA-5). Off-white solid; m.p. 175–177 °C; yield 72%, 0.216 g; ^{1}H NMR (400 MHz, MeOH-d_4): δ 8.29 (d, J = 6.25 Hz 1H), 7.83 (s, 1H), 7.29–7.12 (m, 4H), 6.99 (d, J = 8.1 Hz, 1H), 6.11 (d, J = 14.7 Hz, 1H), 4.10 (d, J = 2.1 Hz 1H), 4.04 (d, J = 2.06 Hz 1H), 3.81 (s, 3H), 3.72 (s, 3H), 3.68 (t, J = 5.3 Hz, 1H), 3.51 (t, J = 5.1 Hz, 1H), 3.39–3.31 (m, 2H), 2.41 (d, J = 13.1 Hz, 1H), 2.23–2.09 (m, 2H), 1.92–1.87 (m, 2H), 1.82–1.79 (m, 2H), 1.45–1.49 (m, 4H). ^{13}C NMR (101 MHz, DMSO-d_6): δ 162.34, 160.27, 156.34, 150.26, 149.62, 135.93, 131.47, 129.82, 128.34, 124.36, 122.56, 120.53, 119.42, 117.63, 115.72, 113.64, 58.34, 57.62, 47.39, 45.76, 31.52, 27.43, 26.39. ESI MS (*m*/*z*): calcd for $C_{27}H_{31}N_3O_3$ 445.55; found 446.1 $[M + H]^+$. Anal. calcd for $C_{27}H_{31}N_3O_3$ (%): C, 72.78; H, 7.01; N, 9.43; O, 10.77; found: C, 72.70; H, 7.08; N, 9.40; O, 10.80.

(4-(2-(3,4-Dimethoxyphenyl)-imidazo[1,2-*a*]pyridin-6-yl)-5,6-dihydropyridin-1(2*H*)-yl)(phenyl)-methanone (IPA-6). Off-white solid; m.p. 116–118 °C; yield 74%, 0.220 g; ^{1}H NMR (400 MHz, DMSO-d_6): δ 8.51 (s, 1H), 8.26 (s, 1H), 7.55–7.47 (m, 9H), 7.01 (d, J = 8.4 Hz, 1H), 6.37–6.19 (bs, 1H), 4.30 (bs, 1H), 4.10 (bs, 1H), 3.84 (s, 4H), 3.79 (s, 3H), 3.55 (s, 1H), 2.57 (s, 2H). ^{13}C NMR (101 MHz, DMSO-d_6): δ 149.42, 149.14, 145.35, 144.41, 139.86, 133.61, 131.65, 129.80, 128.41, 127.48, 127.19, 125.78, 125.04, 123.16, 122.84, 121.53, 120.42, 118.45, 116.42, 112.50, 109.65, 109.28, 56.42, 55.82, 44.63, 42.87, 39.38. ESI MS (*m*/*z*):

calcd for $C_{27}H_{25}N_3O_3$, 439.51; found 440.1 $[M + H]^+$. Anal. calcd for $C_{27}H_{25}N_3O_3$ (%): C, 73.79; H, 5.73; N, 9.56; O, 10.92; found: C, 73.75; H, 5.79; N, 9.50; O, 10.90.

(4-(2-(3,4-Dimethoxyphenyl)-imidazo[1,2-*a*]pyridin-6-yl)-5,6-dihydropyridin-1(2*H*)-yl)(p-tolyl)-methanone (IPA-7). Off-white solid; m.p. 130–1328 °C; yield 71%, 0.218 g; ^{1}H NMR (400 MHz, DMSO-d_6): δ 8.30 (s, 1H), 7.96 (s, 1H), 7.42–7.33 (m, 4H), 7.28 (d, J = 8.0 Hz, 2H), 7.21 (d, J = 7.2 Hz, 1H), 6.90 (d, J = 8.4 Hz, 1H), 6.22–6.02 (bs, 1H), 4.28 (bs, 1H), 4.09 (bs, 1H), 3.90 (bs, 1H), 3.82 (s, 3H), 3.76 (s, 3H), 3.58 (s, 1H), 2.52 (s, 2H), 2.30 (s, 3H). ^{13}C NMR (101 MHz, DMSO-d_6): δ 151.42, 149.87, 146.37, 144.89, 139.86, 133.61, 131.65, 129.80, 129.41, 127.48, 127.19, 125.78, 125.00, 123.16, 122.84, 121.53, 118.45, 116.42, 112.50, 109.65, 109.28, 56.02, 55.95, 43.71, 40.63, 39.38, 21.40. ESI MS (m/z): calcd for $C_{28}H_{27}N_3O_3$, 453.53; found 454.2 $[M + H]^+$. Anal. calcd for $C_{28}H_{27}N_3O_3$ (%): C, 74.15; H, 6.00; N, 9.27; O, 10.58; found: C, 74.10; H, 6.05; N, 9.22; O, 10.62.

(4-(2-(3,4-Dimethoxyphenyl)-imidazo[1,2-*a*]pyridin-6-yl)-5,6-dihydropyridin-1(2*H*)-yl)(4-fluorophenyl)-methanone (IPA-8). Off-white solid; m.p. 118–119 °C; yield 73%, 0.225 g; ^{1}H NMR (400 MHz, MeOH-d_4): δ 8.35 (s, 1H), 8.00 (s, 1H), 7.47–7.41 (m, 4H), 7.36 (dd, J = 2.0 Hz, 7.6 Hz, 2H), 7.14 (t, J = 8.4 Hz, 2H), 6.92 (d, J = 8.4 Hz, 1H), 6.24–6.05 (bs, 1H), 4.30 (bs, 1H), 4.1 (bs, 1H), 3.92 (bs, 1H), 3.83 (s, 3H), 3.77 (s, 3H), 3.59 (s, 1H), 2.56 (s, 2H). ^{13}C NMR (101 MHz, DMSO-d_6): δ 164.36, 161.91, 149.42, 149.21, 144.99, 144.21, 132.93, 131.60, 130.00, 126.85, 125.15, 123.45, 122.92, 121.51, 118.50, 116.24, 116.02, 115.81, 112.50, 109.66, 109.35, 56.02, 55.97, 45.36, 43.87, 31.58. ESI MS (m/z): calcd for $C_{27}H_{24}FN_3O_3$, 457.50; found 458.2 $[M + H]^+$. Anal. calcd for $C_{27}H_{24}FN_3O_3$ (%): C, 70.88; H, 5.29; F, 4.15; N, 9.18; O, 10.49; found: C, 70.80; H, 5.28; F, 4.11; N, 9.15; O, 10.50.

(4-Chlorophenyl)(4-(2-(3,4-dimethoxyphenyl)-imidaz-*o*[1,2-*a*]pyridin-6-yl)-5,6-dihydropyridin-1(2*H*)-yl)-methanone (IPA-9). Pale yellow solid; m.p. 137–139 °C; yield 72%, 0.23 g; ^{1}H NMR (400 MHz, MeOH-d_4): δ 8.31 (s, 1H), 7.96 (s, 1H), 7.42–7.38 (m, 4H), 7.31 (dd, J = 1.9 Hz, 7.1 Hz, 2H), 7.10 (t, J = 8.2 Hz, 2H), 6.91 (d, J = 8.3 Hz, 1H), 6.21–6.07 (bs, 1H), 4.29 (bs, 1H), 4.08 (bs, 1H), 3.90 (bs, 1H), 3.84 (s, 3H), 3.79 (s, 3H), 3.56 (s, 1H), 2.53 (s, 2H). ^{13}C NMR (101 MHz, DMSO-d_6): δ 164.35, 161.91, 149.42, 149.21, 144.99, 144.21, 132.93, 131.60, 130.00, 126.85, 125.15, 123.45, 122.92, 121.51, 118.50, 116.24, 116.02, 115.81, 112.50, 109.66, 109.35, 56.02, 55.97, 45.36, 43.87, 32.80. ESI MS (m/z): calcd for $C_{27}H_{24}ClN_3O_3$, 473.95; found 474.1 $[M + H]^+$. Anal. calcd for $C_{27}H_{24}ClN_3O_3$ (%): C, 68.42; H, 5.10; Cl, 7.48; N, 8.87; O, 10.13; found: C, 68.40; H, 5.15; Cl, 7.40; N, 8.85; O, 10.10.

(4-(2-(3,4-Dimethoxyphenyl)-imidazo[1,2-*a*]pyridin-6-yl)-5,6-dihydropyridin-1(2*H*)-yl)(2-fluorophenyl)-methanone (IPA-10). Pale yellow solid; m.p. 112–114 °C; yield 75%, 0.23 g; ^{1}H NMR (400 MHz, DMSO-d_6): δ 8.36 (s, 1H), 8.12 (s, 1H), 7.99–7.86 (m, 2H), 7.47 (dd, J = 2.0 Hz, 7.6 Hz, 2H), 7.14 (t, J = 8.4 Hz, 2H), 6.92 (d, J = 8.38 Hz, 2H), 6.24–6.05 (bs, 1H), 4.30 (bs, 1H), 4.1 (bs, 1H), 3.92 (bs, 1H), 3.83 (s, 3H), 3.77 (s, 3H), 3.59 (s, 1H), 2.56 (s, 2H). ^{13}C NMR (101 MHz, DMSO-d_6): δ 163.29, 162.93, 149.76, 149.83, 145.72, 144.27, 133.47, 132.74, 131.65, 127.85, 125.85, 123.49, 122.73, 121.58, 118.72, 116.93, 115.72, 114.85, 112.57, 109.63, 108.35, 56.72, 55.47, 45.31, 43.92, 31.47. ESI MS (m/z): calcd for $C_{27}H_{24}FN_3O_3$, 457.5; found 458.1 $[M + H]^+$. Anal. calcd for $C_{27}H_{24}FN_3O_3$ (%): C, 70.88; H, 5.29; F, 4.15; N, 9.18; O, 10.49; found: C, 70.85; H, 5.22; F, 4.15; N, 9.10; O, 10.57.

(4-(2-(3,4-Dimethoxyphenyl)-imidazo[1,2-*a*]pyridin-6-yl)-5,6-dihydropyridin-1(2*H*)-yl)(3-fluorophenyl)-methanone (IPA-11). Pale yellow solid; m.p. 109–111 °C; yield 71%, 0.22 g; ^{1}H NMR (400 MHz, DMSO-d_6): δ 8.56 (s, 1H), 8.25 (s, 1H), 7.59–7.51 (m, 5H), 7.49–7.30 (m, 3H), 7.02 (d, J = 8.8 Hz, 1H), 6.37–6.19 (bs, 1H), 4.30 (bs, 1H), 4.09 (bs, 1H), 3.84 (bs, 4H), 3.79 (s, 4H), 3.54 (s, 1H), 2.58 (s, 2H). ^{13}C NMR (101 MHz, DMSO-d_6): δ 162.74, 161.92, 151.74, 150.82, 146.79, 144.58, 134.67, 132.74, 131.65, 127.85, 125.85, 123.49, 122.73, 121.58, 118.72, 116.93, 115.72, 114.85, 112.31, 109.45, 107.14, 56.82, 55.73, 45.96, 43.58, 31.42. ESI MS (m/z): calcd for $C_{27}H_{24}FN_3O_3$ 457.5; found 458.1 $[M + H]^+$. Anal. calcd for $C_{27}H_{24}FN_3O_3$ (%): C, 70.88; H, 5.29; F, 4.15; N, 9.18; O, 10.49; found: C, 70.85; H, 5.22; F, 4.10; N, 9.23; O, 10.40.

(4-(2-(3,4-Dimethoxyphenyl)-imidazo[1,2-*a*]pyridin-6-yl)-5,6-dihydropyridin-1(2*H*)-yl)(3-(trifluoromethyl)-phenyl)-methanone (IPA-12). Off-white solid; m.p. 119–121 °C; yield 71%, 0.24 g; ^{1}H NMR (400 MHz, DMSO-d_6): δ 8.51 (s, 1H), 8.27 (s, 1H), 7.96–7.65 (m, 4H), 7.62–7.38 (m, 4H), 7.02 (d, J = 8.5 Hz, 1H), 6.28 (d, J = 78.9 Hz, 1H), 4.33 (s, 1H), 4.09 (s, 1H), 3.96–3.72 (m, 7H), 3.54 (s, 1H), 2.59 (s, 2H). ^{13}C NMR (101 MHz, DMSO-d_6): δ 149.42, 149.14, 145.35, 144.41, 137.63, 131.62, 130.21, 127.17, 126.79, 125.73, 124.92, 124.11, 123.13, 123.02, 122.88, 121.16, 118.45, 116.43, 112.49, 109.64, 109.30, 56.01, 55.94, 44.37, 42.68, 27.05. ESI MS (m/z): calcd for $C_{28}H_{24}F_3N_3O_3$ 507.5; found 508.1 $[M + H]^+$. Anal. calcd for $C_{28}H_{24}F_3N_3O_3$ (%): C, 66.27; H, 4.77; F, 11.23; N, 8.28; O, 9.46; found: C, 66.20; H, 4.75; F, 11.20; N, 8.22; O, 9.50.

(4-(2-(3,4-Dimethoxyphenyl)-imidazo[1,2-*a*]pyridin-6-yl)-5,6-dihydropyridin-1(2*H*)-yl)(pyridin-2-yl)-methanone (IPA-13). Off-white solid; m.p. 117–119 °C; yield 72%, 0.24 g; ^{1}H NMR (400 MHz, DMSO-d_6): δ 8.69 (d, J = 7.6 Hz, 1H), 8.37 (d, J = 6.8 Hz, 2H), 8.17 (s, 1H), 8.13 (t, J = 8.2 Hz, 1H), 7.98 (t, J = 7.8 Hz, 1H), 7.54 (d, J = 7.4 Hz, 1H), 7.32 (s, 1H), 7.18–7.12 (m, 2H), 6.98 (d, J = 7.2 Hz, 1H), 6.37–6.24 (bs, 1H), 4.32 (bs, 1H), 4.21 (bs, 1H), 3.94 (t, J = 5.6 Hz, 1H), 3.84 (s, 3H), 3.78 (s, 3H), 3.64 (t, J = 5.6 Hz, 1H), 2.59 (d, J = 13.2 Hz, 2H). ^{13}C NMR (101 MHz, DMSO-d_6): δ 152.63, 149.17, 146.37, 145.38, 138.69, 132.67, 131.25, 128.17, 127.76, 126.78, 125.93, 124.87, 123.64, 122.93, 121.88, 120.17, 119.47, 117.45, 113.45, 110.64, 109.30, 56.34, 55.91, 44.38, 42.73, 27.83. ESI MS (m/z): calcd for $C_{24}H_{28}N_4O_3S$, 440.49; found 441.1 $[M + H]^+$. Anal. calcd for $C_{24}H_{28}N_4O_3S$ (%): C, 70.89; H, 5.49; N, 12.72; O, 10.90; found: C, 70.80; H, 5.58; N, 12.70; O, 10.92.

(4-(2-(3,4-Dimethoxyphenyl)-imidazo[1,2-*a*]pyridin-6-yl)-5,6-dihydropyridin-1(2*H*)-yl)(thiophen-2-yl)-methanone (IPA-14). Pale yellow solid; m.p. 112–114 °C; yield 78%, 0.35 g; ^{1}H NMR (400 MHz, DMSO-d_6): δ 8.52 (s, 1H), 8.27 (s, 1H), 7.80 (d, J = 4.8 Hz, 1H), 7.54–7.47 (m, 5H), 7.17 (t, J = 4.8 Hz, 1H),

7.01 (d, J = 8.4 Hz, 1H), 6.31 (bs, 1H), 4.37 (bs, 2H), 3.87 (d, J = 5.2 Hz, 2H), 3.84 (s, 3H), 3.79 (s, 3H), 2.63 (s, 2H). ^{13}C NMR (101 MHz, DMSO-d_6): δ 159.27, 150.47, 149.36, 147.58, 146.87, 144.82, 132.63, 127.56, 125.94, 123.98, 122.85, 121.78, 119.42, 117.43, 116.92, 113.74, 112.85, 110.64, 109.29, 56.87, 55.93, 44.38, 42.73, 29.83. ESI MS (m/z): calcd for $C_{25}H_{23}N_3O_3S$, 445.53; found 446.1 $[M + H]^+$. Anal. calcd for $C_{25}H_{23}N_3O_3S$ (%): C, 67.40; H, 5.20; N, 9.43; O, 10.77; S, 7.20; found: C, 67.10; H, 5.60; N, 9.42; O, 10.75; S, 7.15.

(4-(2-(3,4-Dimethoxyphenyl)-imidazo[1,2-*a*]pyridin-6-yl)-5,6-dihydropyridin-1(2*H*)-yl)(furan-2-yl)-methanone (IPA-15). Off-white solid; m.p. 108–110 °C; yield 72%, 0.24 g; ^{1}H NMR (400 MHz, DMSO-d_6): δ 8.51 (s, 1H), 8.26 (s, 1H), 7.89 (d, J = 1.0 Hz, 1H), 7.65–7.36 (m, 4H), 7.08 (d, J = 3.3 Hz, 1H), 7.02 (d, J = 8.4 Hz, 1H), 6.67 (dd, J = 3.4, 1.7 Hz, 1H), 6.30 (s, 1H), 4.36 (s, 2H), 3.89 (s, 2H), 3.85 (s, 3H), 3.79 (s, 3H), 2.62 (s, 2H). ^{13}C NMR (101 MHz, DMSO-d_6): δ 158.97, 149.42, 149.14, 147.58, 145.33, 144.41, 131.69, 127.17, 124.96, 123.18, 122.86, 121.45, 118.46, 116.42, 115.97, 112.49, 111.83, 109.64, 109.29, 56.01, 55.95, 44.36, 42.78, 29.46. ESI MS (m/z): calcd for $C_{25}H_{23}N_3O_4$, 429.47; found 430.2 $[M + H]^+$. Anal. calcd for $C_{25}H_{23}N_3O_4$ (%): C, 69.92; H, 5.40; N, 9.78; O, 14.90; found: C, 69.90; H, 5.45; N, 9.72; O, 14.90.

(4-(2-(3,4-Dimethoxyphenyl)-imidazo[1,2-*a*]pyridin-6-yl)-5,6-dihydropyridin-1(2*H*)-yl)(oxazol-4-yl)-methanone (IPA-16). Off-white solid; m.p. 113–115 °C; yield 84%, 0.24 g; ^{1}H NMR (400 MHz, DMSO-d_6): δ 8.64 (s, 1H), 8.56 (s, 1H), 8.53 (s, 1H), 8.26 (s, 1H), 7.54–7.47 (m, 4H), 7.01 (d, J = 8.0 Hz, 1H), 6.35–6.31 (bs, 1H), 4.60 (s, 1H), 4.28 (s, 1H), 4.08 (s, 1H), 3.84 (s, 4H), 3.79 (s, 3H), 2.62 (d, J = 16.4 Hz, 2H). ^{13}C NMR (101 MHz, DMSO-d_6): δ 159.25, 151.45, 149.83, 148.52, 146.73, 142.71, 130.69, 126.27, 125.26, 123.57, 122.86, 121.45, 117.59, 116.47, 115.93, 113.47, 110.82, 109.67, 109.27, 56.31, 55.96, 44.39, 43.72, 28.43. ESI MS (m/z): calcd for $C_{24}H_{22}N_4O_4$ 430.46; found 431.1 $[M + H]^+$. Anal. calcd for $C_{24}H_{22}N_4O_4$ (%): C, 66.97; H, 5.15; N, 13.02; O, 14.87; found: C, 66.94; H, 5.10; N, 13.10; O, 14.85.

2-(Benzyloxy)-1-(4-(2-(3,4-dimethoxyphenyl)-imidazo[1,2-*a*]pyridin-6-yl)-5,6-dihydropyridin-1(2*H*)-yl)-ethanone (IPA-17). Off-white solid; m.p. 154–156 °C; yield 81%, 0.265 g; ^{1}H NMR (400 MHz, DMSO-d_6): δ 8.49 (d, J = 10.8 Hz, 1H), 8.27 (s, 1H), 7.55–7.49 (m, 4H), 7.44–7.31 (m, 5H), 7.01 (d, J = 8.4.0 Hz, 1H), 6.30–6.26 (bs, 1H), 4.54 (d, J = 6.4 Hz, 2H), 4.28 (d, J = 15.2 Hz, 2H), 4.14 (s, 2H), 3.85 (s, 3H), 3.79 (s, 3H), 3.71 (d, J = 5.2 Hz, 1H), 3.63 (s, 1H), 2.54 (s, 2H). ^{13}C NMR (100.61 MHz, DMSO-d_6): δ 168.26, 150.93, 149.17, 148.34, 145.74, 138.12136.25, 133.62, 131.45, 129.61, 129.01, 126.32, 124.82, 121.98, 116.27, 113.52, 111.97, 110.45, 79.18, 61.15, 53.81, 51.34, 49.58, 45.32, 28.12. ESI MS (m/z): calcd for $C_{29}H_{29}N_3O_4$ 483.56; found 484.47 $[M + H]^+$. Anal. calcd for $C_{29}H_{29}N_3O_4$ (%): C, 72.03; H, 6.05; N, 8.69; O, 13.23; found: C, 72.02; H, 6.10; N, 8.65; O, 13.25.

2-(3,4-Dimethoxyphenyl)-6-(1-(methylsulfonyl)-1,2,3,6-tetrahydropyridin-4-yl)-imidazo[1,2-*a*]pyridine (IPS-1). Off-white solid; m.p. 229–231 °C; yield 79%, 0.22 g; ^{1}H NMR (400 MHz, DMSO-d_6): δ 8.46 (s, 1H), 8.25 (s, 1H), 7.53–7.45 (m, 4H), 7.01 (d, J = 8.4 Hz, 1H), 6.27 (s, 1H), 3.84 (s, 3H), 3.79 (s, 1H), 3.03 (d, J = 2.8 Hz, 2H), 2.58 (t, J = 5.6 Hz, 2H), 2.28 (s, 3H). ^{13}C NMR (101 MHz, DMSO-d_6): δ 149.18, 148.35, 146.32, 145.72, 132.67, 128.93, 125.96, 124.37, 123.49, 121.85, 118.46, 116.43, 112.50, 109.64, 109.30, 56.02, 55.96, 44.99, 43.46, 42.51, 40.86. ESI MS (m/z): calcd for $C_{21}H_{23}N_3O_4S$, 413.49; found 414.1 $[M + H]^+$. Anal. calcd for $C_{21}H_{23}N_3O_4S$ (%): C, 61.00; H, 5.61; N, 10.16; O, 15.48; S, 7.75; found: C, 61.05; H, 5.60; N, 10.12; O, 15.45; S, 7.70.

2-(3,4-Dimethoxyphenyl)-6-(1-(ethylsulfonyl)-1,2,3,6-tetrahydropyridin-4-yl)-imidazo[1,2-*a*]pyridine (IPS-2). Off-white solid; m.p. 233–235 °C; yield 83%, 0.24 g; ^{1}H NMR (400 MHz, DMSO-d_6): δ 8.51 (s, 1H), 8.27 (s, 1H), 7.65–7.41 (m, 4H), 7.02 (d, J = 8.5 Hz, 1H), 6.30 (s, 1H), 3.94 (d, J = 2.7 Hz, 2H), 3.85 (s, 3H), 3.80 (s, 3H), 3.47 (t, J = 5.7 Hz, 2H), 3.13 (q, J = 7.4 Hz, 2H), 2.59 (s, 2H), 1.24 (t, J = 7.4 Hz, 3H). ^{13}C NMR (101 MHz, DMSO-d_6): δ 149.82, 149.15, 145.36, 144.42, 131.35, 127.16, 124.90, 123.15, 122.92, 120.85, 118.46, 116.43, 112.50, 109.64, 109.30, 56.02, 55.96, 44.99, 43.46, 42.51, 26.86, 8.04. ESI MS (m/z): calcd for $C_{22}H_{25}N_3O_4S$ 427.52; found 428.2 $[M + H]^+$. Anal. calcd for $C_{22}H_{25}N_3O_4S$ (%): C, 61.81; H, 5.89; N, 9.83; O, 14.97; S, 7.50; found: C, 61.80; H, 5.90; N, 9.82; O, 14.95; S, 7.55.

2-(3,4-Dimethoxyphenyl)-6-(1-(propylsulfonyl)-1,2,3,6-tetrahydropyridin-4-yl)-imidazo[1,2-*a*]pyridine (IPS-3). Off-white solid; m.p. 245–247 °C; yield 77%, 0.23 g; ^{1}H NMR (400 MHz, MeOH-d_4): δ 8.67 (s, 1H), 8.33 (s, 1H), 8.03 (d, J = 9.6 Hz, 1H), 7.73 (d, J = 9.2 Hz, 1H), 7.36 (d, J = 8.0 Hz, 2H), 7.04 (d, J = 8.4 Hz, 2H), 6.37 (s, 1H), 3.96 (d, J = 2.4 Hz, 2H), 3.85 (s, 3H), 3.81 (s, 3H), 3.66–3.61 (m, 1H), 3.50 (t, J = 5.6 Hz, 2H), 3.16–3.10 (m, 1H), 2.99 (t, J = 7.6 Hz, 2H), 2.61 (s, 2H), 1.78–1.72 (m, 2H), 0.98 (t, J = 3.6 Hz, 3H). ^{13}C NMR (100.61 MHz, DMSO-d_6): δ 150.42, 149.75, 146.38, 144.92, 132.84, 128.35, 125.96, 124.75, 123.92, 121.85, 119.43, 117.36, 114.56, 110.64, 109.32, 61.79, 56.84, 55.87, 46.72, 44.76, 43.56, 13.89, 12.56. ESI MS (m/z): calcd for $C_{23}H_{27}N_3O_4S$, 441.54; found 442.2 $[M + H]^+$. Anal. calcd for $C_{23}H_{27}N_3O_4S$ (%); C, 62.56; H, 6.16; N, 9.52; O, 14.49; S, 7.26; found: C, 62.50; H, 6.12; N, 9.55; O, 14.48; S, 7.28.

6-(1-(Cyclopropylsulfonyl)-1,2,3,6-tetrahydropyridin-4-yl)-2-(3,4dimethoxyphenyl)-imidazo[1,2-*a*]pyridine (IPS-4). Brown solid; m.p. 101–103 °C; yield 76%, 0.225 g; ^{1}H NMR (400 MHz, DMSO-d_6): δ 8.52 (s, 1H), 8.28 (s, 1H), 7.54 (dd, J = 5.6, 1.6 Hz, 2H), 7.47 (dd, J = 5.6, 1.6 Hz, 2H), 7.02 (d, J = 8.4 Hz, 1H), 6.32 (bs, 1H), 3.96 (d, J = 2.0 Hz, 2H), 3.84 (s, 3H), 3.79 (s, 3H), 3.48 (t, J = 5.6 Hz, 2H), 2.69 (t, J = 6.4 Hz, 1H), 2.62 (s, 2H), 0.99 (m, 4H). ^{13}C NMR (100.61 MHz, DMSO-d_6): δ 150.32, 149.38, 147.92, 145.91, 132.84, 128.35, 125.96, 124.75, 123.92, 121.85, 119.43, 117.36, 114.56, 110.64, 109.39, 61.78, 56.34, 55.86, 46.59, 44.78, 43.52, 38.27, 4.36. ESI MS (m/z): calcd for $C_{23}H_{25}N_3O_4S$, 439.53; found 440.1 $[M + H]^+$. Anal. calcd for $C_{23}H_{25}N_3O_4S$ (%): C, 62.85; H, 5.73; N, 9.56; O, 14.56; S, 7.29; found: C, 62.80; H, 5.75; N, 9.50; O, 14.50; S, 7.25.

6-(1-(Cyclopentylsulfonyl)-1,2,3,6-tetrahydropyridin-4-yl)-2-(3,4-dimethoxyphenyl)-imidazo[1,2-*a*]pyridine (IPS-5). Off-white solid; m.p. 105–107 °C; yield 75%, 0.23 g; ^{1}H NMR (400

MHz, MeOH-d_4): δ 8.31 (s, 1H), 7.98 (s, 1H), 7.42–7.34 (m, 4H), 6.92 (d, J = 8.4 Hz 1H), 6.16 (s, 1H), 3.94 (d, J = 2.8 Hz 2H), 3.83 (s, 3H), 3.77 (s, 3H), 3.59 (t, J = 8.0 Hz, 1H), 3.49 (t, J = 5.6 Hz, 2H), 2.53 (s, 2H), 1.94–1.85 (m, 4H), 1.69–1.67 (m, 2H), 1.58–1.55 (m, 2H). ^{13}C NMR (101 MHz, DMSO-d_6): δ 150.42, 149.36, 145.39, 144.72, 131.48, 127.96, 124.36, 123.74, 122.84, 121.27, 118.45, 116.49, 112.56, 109.64, 109.37, 60.15, 56.72, 55.95, 45.18, 42.80, 29.45, 27.23, 26.65. ESI MS (m/z): calcd for $C_{25}H_{29}N_3O_4S$, 467.58; found 468.1 $[M + H]^+$. Anal. calcd for $C_{25}H_{29}N_3O_4S$ (%): C, 64.22; H, 6.25; N, 8.99; O, 13.69; S, 6.86; found: C, 64.20; H, 6.25; N, 8.90; O, 13.75; S, 6.85.

6-(1-(Cyclohexylsulfonyl)-1,2,3,6-tetrahydropyridin-4-yl)-2-(3,4-dimethoxyphenyl)-imidazo[1,2-*a*]pyridine (IPS-6). Off-white solid; m.p. 113–115 °C; yield 87%, 0.44 g; ^{1}H NMR (400 MHz, MeOH-d_4): δ 8.30 (s, 1H), 7.97 (s, 1H), 7.42–7.34 (m, 4H), 6.91 (d, J = 8.4 Hz 1H), 6.15 (s, 1H), 3.96 (d, J = 2.4 Hz 2H), 3.83 (s, 3H), 3.77 (s, 3H), 3.51 (t, J = 5.6 Hz, 2H), 3.06–3.00 (m, 1H), 2.51 (s, 2H), 2.03 (d, J = 11.2 Hz 2H), 1.79 (d, J = 11.6 Hz, 2H), 1.61 (d, J = 12.0 Hz, 1H), 1.46–1.36 (m, 2H), 1.30–1.24 (m, 3H). ^{13}C NMR (101 MHz, DMSO-d_6): δ 149.42, 149.14, 145.35, 144.42, 131.42, 127.18, 124.97, 123.13, 122.88, 121.22, 118.45, 116.44, 112.50, 109.64, 109.30, 60.12, 56.02, 55.95, 45.18, 42.80, 27.23, 26.65, 25.29, 24.97. ESI MS (m/z): calcd for $C_{26}H_{31}N_3O_4S$, 481.61; found 482.2 $[M + H]^+$. Anal. calcd for $C_{26}H_{31}N_3O_4S$ (%): C, 64.84; H, 6.49; N, 8.73; O, 13.29; S, 6.66; found: C, 64.85; H, 6.45; N, 8.70; O, 13.25; S, 6.60.

2-(3,4-Dimethoxyphenyl)-6-(1-(phenylsulfonyl)-1,2,3,6-tetrahydropyridin-4-yl)-imidazo[1,2-*a*]pyridine (IPS-7). Pale yellow solid; m.p. 130–132 °C; yield 73%, 0.36 g; ^{1}H NMR (400 MHz, DMSO-d_6): δ 8.45 (s, 1H), 8.26 (s, 1H), 7.84 (dd, J = 7.2, 3.0 Hz, 2H), 7.69 (d, J = 13.6 Hz 1H), 7.65 (d, J = 7.2 Hz, 2H), 7.53–7.46 (m, 3H), 7.38 (d, J = 9.6 Hz 1H), 7.01 (d, J = 8.4 Hz 1H), 6.21 (s, 1H), 3.84 (s, 3H), 3.78 (s, 3H), 3.71 (s, 2H), 3.26 (t, J = 5.6 Hz 2H), 2.56 (s, 2H). ^{13}C NMR (101 MHz, DMSO-d_6): δ 150.42, 149.72, 147.56, 144.98, 139.72, 135.42, 132.26, 131.08, 129.97, 127.93, 125.76, 124.47, 122.76, 120.97, 119.42, 116.31, 113.45, 110.64, 109.32, 56.12, 55.85, 45.89, 43.15, 26.39. ESI MS (m/z): calcd for $C_{26}H_{25}N_3O_4S$, 475.56; found 486.1 $[M + H]^+$. Anal. calcd for $C_{26}H_{25}N_3O_4S$ (%): C, 65.67; H, 5.30; N, 8.84; O, 13.46; S, 6.74; found: C, 65.65; H, 5.32; N, 8.80; O, 13.51; S, 6.70.

2-(3,4-Dimethoxyphenyl)-6-(1-tosyl-1,2,3,6-tetrahydropyridin-4-yl)-imidazo[1,2-*a*]pyridine (IPS-8). Brown solid; m.p. 90–92 °C; yield 78%, 0.26 g; ^{1}H NMR (400 MHz, DMSO-d_6): δ 8.44 (s, 1H), 8.27 (s, 1H), 7.76 (d, J = 8.4 Hz, 2H), 7.68 (d, J = 8.8 Hz, 2H), 7.55–7.47 (m, 3H), 7.38 (d, J = 8.8 Hz, 1H), 7.03 (d, J = 8.4 Hz, 1H), 6.22 (s, 1H), 3.84 (s, 3H), 3.79 (s, 3H), 3.72 (s, 2H), 3.26 (t, J = 5.6 Hz, 2H), 2.56 (s, 2H), 2.29 (s, 3H). ^{13}C NMR (101 MHz, DMSO-d_6): δ 150.12, 149.26, 145.97, 143.78, 137.54, 134.58, 131.29, 130.56, 129.88, 126.53, 124.16, 123.54, 122.34, 119.24, 117.49, 116.37, 112.45, 109.64, 108.38, 56.73, 55.92, 45.69, 43.18, 28.36, 21.73. ESI MS (m/z): calcd for $C_{27}H_{27}N_3O_4S$, 489.59; found 490.2 $[M + H]^+$. Anal. calcd for $C_{27}H_{27}N_3O_4S$ (%): C, 66.24; H, 5.56; N, 8.58; O, 13.07; S, 6.55; found: C, 66.20; H, 5.60; N, 8.50; O, 13.18; S, 6.50.

2-(3,4-Dimethoxyphenyl)-6-(1-((4-fluorophenyl)-sulfonyl)-1,2,3,6-tetrahydropyridin-4-yl)-imidazo[1,2-*a*]pyridine (IPS-9). Off-white solid; m.p. 97–99 °C; yield 83%, 0.27 g; ^{1}H NMR (400 MHz, DMSO-d_6): δ 8.46 (s, 1H), 8.26 (s, 1H), 7.93–7.90 (m, 2H), 7.53–7.46 (m, 5H), 7.39 (d, J = 9.6 Hz 1H), 7.01 (d, J = 8.4 Hz, 1H), 6.23 (s, 1H), 3.84 (s, 3H), 3.79 (s, 3H), 3.72 (s, 2H), 3.27 (t, J = 5.6 Hz, 2H), 2.57 (s, 2H). ^{13}C NMR (101 MHz, DMSO-d_6): δ 162.48, 150.42, 149.73, 146.29, 144.87, 138.85, 135.76, 132.74, 131.26, 129.84, 127.93, 125.76, 123.86, 122.74, 120.94, 119.58, 117.38, 113.49, 110.68, 109.37, 56.12, 55.94, 45.25, 43.93, 28.46. ESI MS (m/z): calcd for $C_{26}H_{24}FN_3O_4S$, 493.55; found 494.1 $[M + H]^+$. Anal. calcd for $C_{26}H_{24}FN_3O_4S$ (%): C, 66.24; H, 5.56; N, 8.58; O, 13.07; S, 6.55; found: C, 66.20; H, 5.53; N, 8.50; O, 10.07; S, 6.58.

6-(1-((4-Chlorophenyl)-sulfonyl)-1,2,3,6-tetrahydropyridin-4-yl)-2-(3,4dimethoxyphenyl)-imidazo[1,2-*a*]pyridine (IPS-10). Off-white solid; m.p. 102–104 °C; yield 83%, 0.27 g; ^{1}H NMR (400 MHz, DMSO-d_6) δ 8.45 (s, 1H), 8.26 (s, 1H), 7.85 (d, J = 8.6 Hz, 2H), 7.73 (d, J = 8.6 Hz, 2H), 7.50 (dd, J = 10.1, 7.7, 1.8 Hz, 3H), 7.38 (dd, J = 9.6, 1.6 Hz, 1H), 7.01 (d, J = 8.4 Hz, 1H), 6.20 (s, 1H), 3.85 (s, 3H), 3.79 (s, 3H), 3.73 (s, 2H), 3.28 (t, J = 5.6 Hz, 2H), 2.56 (s, 2H). ^{13}C NMR (101 MHz, DMSO-d_6): δ 149.42, 149.19, 145.19, 144.28, 138.74, 134.99, 131.26, 130.06, 129.87, 126.97, 124.76, 123.25, 122.99, 119.94, 118.48, 116.31, 112.49, 109.64, 109.32, 56.02, 55.95, 45.49, 43.10, 26.49. ESI MS (m/z): calcd for $C_{26}H_{24}ClN_3O_4S$, 510.0; found 511.1 $[M + H]^+$. Anal. calcd for $C_{26}H_{24}ClN_3O_4S$ (%): C, 61.23; H, 4.74; Cl, 6.95; N, 8.24; O, 12.55; S, 6.29; found: C, 61.20; H, 4.78; Cl, 6.90; N, 8.29; O, 12.50; S, 6.20.

6-(1-((4-(*tert*-Butyl)-phenyl)-sulfonyl)-1,2,3,6-tetrahydropyridin-4-yl)-2-(3,4-dimethoxyphenyl)-imidazo[1,2-*a*]pyridine (IPS-11). Off-white solid; m.p. 177–179 °C; yield 83%, 0.23 g; ^{1}H NMR (400 MHz, DMSO-d_6): δ 8.43 (s, 1H), 8.26 (s, 1H), 7.75 (d, J = 8.4 Hz, 2H), 7.66 (d, J = 8.8 Hz, 2H), 7.53–7.45 (m, 3H), 7.36 (d, J = 8.8 Hz, 1H), 7.01 (d, J = 8.4 Hz, 1H), 6.20 (s, 1H), 3.83 (s, 3H), 3.78 (s, 3H), 3.70 (s, 2H), 3.25 (t, J = 5.6 Hz, 2H), 2.55 (s, 2H), 1.28 (s, 9H). ^{13}C NMR (101 MHz, DMSO-d_6) δ 154.82, 150.41, 149.35, 146.39, 144.85, 141.27, 139.88, 132.45, 130.59, 128.97, 127.54, 125.63, 123.54, 122.96, 119.84, 118.45, 116.41, 112.49, 109.62, 109.27, 56.02, 55.94, 45.48, 43.13, 34.28, 31.76, 28.54. ESI MS (m/z): calcd for $C_{30}H_{33}N_3O_4S$, 531.67; found 532.2 $[M + H]^+$. Anal. calcd for $C_{30}H_{33}N_3O_4S$ (%): C, 67.77; H, 6.26; N, 7.90; O, 12.04; S, 6.03; found: C, 67.70; H, 6.34; N, 7.92; O, 12.05; S, 6.00.

1-(4-((4-(2-(3,4-Dimethoxyphenyl)-imidazo[1,2-*a*]pyridin-6-yl)-5,6-dihydropyridin-1(2H)-yl)-sulfonyl)-phenyl)-ethanone (IPS-12). Brown solid; m.p. 129–131 °C; yield 83%, 0.37 g; ^{1}H NMR (400 MHz, DMSO-d_6): δ 8.44 (s, 1H), 8.25 (s, 1H), 8.18 (d, J = 8.4 Hz, 2H), 7.97 (d, J = 8.4 Hz, 2H), 7.50 (dd, J = 10.1, 9.5, 1.6 Hz, 3H), 7.42–7.26 (m, 1H), 7.01 (d, J = 8.4 Hz, 1H), 6.20 (s, 1H), 3.84 (s, 3H), 3.79 (s, 3H), 3.75 (s, 2H), 3.30 (t, J = 5.4 Hz, 2H), 2.64 (s, 3H), 2.57 (s, 2H). ^{13}C NMR (101 MHz, DMSO-d_6): δ 197.82, 149.41, 149.15, 145.39, 144.39, 140.47, 139.84, 131.33, 129.59, 128.31, 127.14, 124.64, 123.09, 122.96, 119.84, 118.45, 116.41, 112.49, 109.62, 109.27, 56.02, 55.94, 45.48, 43.13, 27.51, 26.51. ESI MS (m/z): calcd for $C_{28}H_{27}N_3O_5S$, 517.6; found 518.2 $[M + H]^+$. Anal. calcd for $C_{28}H_{27}N_3O_5S$ (%): C, 64.97; H, 5.26; N, 8.12; O, 15.45; S, 6.19; found: C, 64.90; H, 5.25; N, 8.10; O, 15.40; S, 6.10.

6-(1-((4-Bromophenyl)-sulfonyl)-1,2,3,6-tetrahydropyridin-4-yl)-2-(3,4-dimethoxyphenyl)-imidazo[1,2-*a*]pyridine (IPS-13). Brown solid; m.p. 156–158 °C; yield 83%, 0.37 g; ^{1}H NMR (400 MHz, DMSO-d_6): δ 8.73 (s, 1H), 8.56 (s, 1H), 7.93–7.88 (m, 3H), 7.82–7.77 (m, 3H), 7.58 (s, 1H), 7.54–7.52 (m, 2H), 7.14 (d, J = 8.4 Hz, 1H), 6.37 (s, 1H), 3.87 (s, 3H), 3.83 (s, 3H), 3.76 (s, 2H), 3.31 (t, J = 5.6 Hz, 2H), 2.61 (s, 2H). ^{13}C NMR (101 MHz, DMSO-d_6): δ 150.47, 149.19, 147.56, 145.28, 139.72, 135.28, 132.26, 131.56, 129.87, 127.24, 125.72, 123.25, 121.54, 120.54, 118.98, 116.29, 113.45, 110.64, 109.38, 56.12, 55.95, 45.49, 43.12, 27.43. ESI MS (m/z): calcd for $C_{26}H_{24}BrN_3O_4S$ 554.46; found 555.1 [M + H]$^+$. Anal. calcd for $C_{26}H_{24}BrN_3O_4S$ (%): C, 56.32; H, 4.36; Br, 14.41; N, 7.58; O, 11.54; S, 5.78; found: C, 56.30; H, 4.32; Br, 14.40; N, 7.52; O, 11.55; S, 5.72.

2-(3,4-Dimethoxyphenyl)-6-(1-((4-nitrophenyl)-sulfonyl)-1,2,3,6-tetrahydropyridin-4-yl)-imidazo[1,2-*a*]pyridine (IPS-14). Brown solid; m.p. 195–197 °C; yield 83%, 0.37 g; ^{1}H NMR (400 MHz, DMSO-d_6): δ 8.44 (dd, J = 8.0, 6.1 Hz, 3H), 8.26 (s, 1H), 8.18–8.05 (m, 2H), 7.50 (dd, J = 10.2, 6.4, 1.9 Hz, 3H), 7.39 (dd, J = 9.6, 1.7 Hz, 1H), 7.02 (d, J = 8.5 Hz, 1H), 6.23 (s, 1H), 3.85 (s, 3H), 3.79 (s, 5H), 3.36 (t, J = 5.6 Hz, 2H), 2.59 (s, 2H). ^{13}C NMR (101 MHz, DMSO-d_6): δ 150.55, 149.41, 149.18, 145.26, 144.31, 141.91, 131.33, 129.52, 127.39, 127.01, 125.19, 124.68, 123.21, 123.05, 119.84, 118.46, 116.36, 112.50, 109.63, 109.31, 56.03, 55.95, 45.45, 43.09, 26.45. ESI MS (m/z): calcd for $C_{26}H_{24}N_4O_6S$ 520.56; found 521.2 [M + H]$^+$. Anal. calcd for $C_{26}H_{24}N_4O_6S$ (%): C, 59.99; H, 4.65; N, 10.76; O, 18.44; S, 6.16; found: C, 59.90; H, 4.62; N, 10.78; O, 18.40; S, 6.12.

6-(1-((5-Chlorothiophen-2-yl)-sulfonyl)-1,2,3,6-tetrahydropyridin-4-yl)-2-(3,4-dimethoxyphenyl)-imidazo[1,2-*a*]pyridine (IPS-15). Brown solid; m.p. 173–175 °C; yield 83%, 0.37 g; ^{1}H NMR (400 MHz, DMSO-d_6): δ 8.51 (s, 1H), 7.66 (d, J = 4.0 Hz, 1H), 7.56–7.54 (m, 2H), 7.49–7.45 (m, 2H), 7.39 (d, J = 4.4 Hz, 1H), 7.02 (d, J = 8.4 Hz, 1H), 6.27 (s, 1H), 3.84 (s, 3H), 3.79 (s, 5H), 3.32 (t, J = 5.6 Hz, 2H), 2.61 (s, 2H). ^{13}C NMR (101 MHz, DMSO-d_6): δ 150.26, 149.57, 145.26, 144.29, 137.82, 135.82, 133.52, 131.95, 130.27, 127.43, 126.74, 125.27, 124.52, 123.47, 121.46, 119.89, 118.72, 117.65, 112.32, 110.62, 109.47, 56.84, 55.86, 45.26, 43.95, 42.76, 27.49. ESI MS (m/z): calcd for $C_{24}H_{22}ClN_3O_4S_2$ 516.03; found 517.1 [M + H]$^+$. Anal. calcd for $C_{26}H_{24}N_4O_6S$ (%): C, 55.86; H, 4.30; Cl, 6.87; N, 8.14; O, 12.40; S, 12.43; found: C, 55.85; H, 4.32; Cl, 6.85; N, 8.10; O, 12.45; S, 12.40.

6-(1-((5-Bromothiophen-2-yl)-sulfonyl)-1,2,3,6-tetrahydropyridin-4-yl)-2-(3,4-dimethoxyphenyl)-imidazo[1,2-*a*]pyridine (IPS-16). Brown solid; m.p. 185–187 °C; yield 83%, 0.37 g; ^{1}H NMR (400 MHz, DMSO-d_6): δ 8.50 (s, 1H), 8.29 (s, 1H), 7.60 (d, J = 4.0 Hz, 1H), 7.55 (dd, J = 5.6, 3.8 Hz, 2H), 7.46 (dd, J = 11.0, 8.2, 2.1 Hz, 3H), 7.11–6.97 (m, 1H), 6.26 (s, 1H), 3.85 (s, 3H), 3.80 (s, 5H), 3.69–3.54 (m, 1H), 3.32 (t, J = 5.7 Hz, 2H), 3.19–3.08 (m, 1H), 2.66 (d, J = 17.4 Hz, 2H). ^{13}C NMR (101 MHz, DMSO-d_6): δ 149.43, 149.25, 144.94, 144.14, 136.87, 134.33, 132.55, 131.25, 129.97, 126.73, 126.34, 124.87, 123.52, 123.13, 120.06, 119.84, 118.52, 116.22, 112.52, 109.66, 109.40, 56.04, 55.98, 53.98, 45.59, 43.27, 42.23, 26.45. ESI MS (m/z): calcd for $C_{24}H_{22}BrN_3O_4S_2$ 560.48; found 561.17 [M + H]$^+$. Anal. calcd for $C_{24}H_{22}BrN_3O_4S_2$ (%): C, 51.43; H, 3.96; Br, 14.26; N, 7.50; O, 11.42; S, 11.44; found: C, 51.40; H, 3.95; Br, 14.20; N, 7.55; O, 11.40; S, 11.45.

2-(3,4-Dimethoxyphenyl)-6-(1-((4-(trifluoromethyl)-phenyl)-sulfonyl)-1,2,3,6-tetrahydropyridin-4-yl)-imidazo[1,2-*a*]pyridine (IPS-17). Brown solid; m.p. 107–109 °C; yield 83%, 0.37 g; ^{1}H NMR (400 MHz, DMSO-d_6): δ 8.45 (s, 1H), 8.25 (s, 1H), 8.08–8.02 (m, 4H), 7.53–7.45 (m, 3H), 7.46 (dd, J = 7.6, 2.0 Hz, 1H), 7.01 (d, J = 8.4 Hz, 1H), 6.21 (bs, 1H), 3.84 (s, 3H), 3.79 (s, 5H), 3.35 (s, 2H), 2.57 (s, 2H). ^{13}C NMR (101 MHz, DMSO-d_6): δ 152.82, 150.47, 149.35, 147.32, 145.85, 142.53, 140.54, 133.45, 131.59, 129.27, 127.35, 125.63, 123.54, 122.96, 119.84, 118.45, 116.41, 112.49, 109.62, 109.27, 56.32, 55.98, 46.38, 43.89, 28.53. ESI MS (m/z): calcd for $C_{27}H_{24}F_3N_3O_4S$ 543.56; found 554.2 [M + H]$^+$. Anal. calcd for $C_{27}H_{24}F_3N_3O_4S$ (%): C, 59.66; H, 4.45; F, 10.49; N, 7.73; O, 11.77; S, 5.90; found: C, 59.60; H, 4.451; F, 10.45; N, 7.78; O, 11.75; S, 5.95.

Conflicts of interest

The authors declare that there are no conflicts of interest.

Acknowledgements

KVGCS gratefully acknowledges support from the Council of Scientific and Industrial Research, New Delhi (CSIR) (F.No. 02(392)/21/EMR II), and DST-FIST (F.No. SR/FST/CSI-240/2012), New Delhi, India. He also acknowledges the Central Analytical Laboratory facilities of BITS Pilani Hyderabad Campus. BKK is thankful to the Ministry of Tribal Affairs, Government of India, for providing financial assistance (Award no. 201920-NFST-TEL- 01497). SM thanks BITS-Pilani, Pilani Campus, for providing adequate facilities to do this research.

References

1 M. Urban, V. Šlachtová and L. Brulíková, Small organic molecules targeting the energy metabolism of *Mycobacterium tuberculosis*, *Eur. J. Med. Chem.*, 2020, 113139.

2 D. Bald and A. Koul, Respiratory ATP synthesis: the new generation of mycobacterial drug targets?, *FEMS Microbiol. Lett.*, 2010, **308**, 1–7.

3 S. Kiazyk and T. B. Ball, Tuberculosis (TB): Latent tuberculosis infection: An overview, *Commun. Dis. Rep. CDR Rev.*, 2017, **43**, 62–66.

4 O. K. Onajole, S. Lun, Y. J. Yun, D. Y. Langue, M. Jaskula-Dybka, A. Flores and W. R. Bishai, Design, synthesis, and biological evaluation of novel imidazo [1, 2-a] pyridinecarboxamides as potent anti-tuberculosis agents, *Chem. Biol. Drug Des.*, 2020, **96**, 1362–1371.

5 A. Deep, R. Kaur Bhatia, R. Kaur, S. Kumar, U. Kumar Jain, H. Singh and P. Kishore Deb, Imidazo-[1, 2-a]-pyridine scaffold as prospective therapeutic agents, *Curr. Top. Med. Chem.*, 2017, **17**, 238–250.

6 C. Enguehard-Gueiffier and A. Gueiffier, Recent Progress in the Pharmacology of Imidazo [1, 2-a] pyridines, *Mini-Rev. Med. Chem.*, 2007, **7**, 888–899.

7 A. Berson, V. Descatoire, A. Sutton, D. Fau, B. Maulny, N. Vadrot and D. Pessayre, Toxicity of alpidem, a peripheral benzodiazepine receptor ligand, but not zolpidem, in rat hepatocytes: role of mitochondrial permeability transition and metabolic activation, *J. Pharmacol. Exp. Ther.*, 2001, **299**, 793–800.

8 A. M. Dar and M. A. Gatoo, Synthesis of new steroidal imidazo-[1, 2-a]-pyridines: DNA binding studies, cleavage activity, and *in vitro* cytotoxicity, *Steroids*, 2015, **104**, 163–175.

9 Y. Uemura, S. Tanaka, T. Yuzuriha and S. Ida, Pharmacokinetic study of loprinone hydrochloride, a new cardiotonic agent, in beagle dogs, *J. Pharm. Pharmacol.*, 1993, **45**(12), 1077–1081.

10 L. Celli, F. Clementi and C. Santagostino, Effect of zolimidine, a derivative of imidazo-(1,2-a)-pyridine, on the gastric mucosa of patients with gastric disorders, *Curr. Ther. Res. Clin. Exp.*, 1975, **18**, 105–123.

11 S. Chitti, S. Singireddi, P. S. K. Reddy, P. Trivedi, Y. Bobde, C. Kumar and K. V. G. C. Sekhar, Design, synthesis and biological evaluation of 2-(3, 4-dimethoxyphenyl)-6 (1, 2, 3, 6-tetrahydropyridin-4-yl)-imidazo-[1, 2-a]-pyridine analogues as antiproliferative agents, *Bioorg. Med. Chem. Lett.*, 2019, **29**, 2551–2558.

12 S. Kang, R. Y. Kim, M. J. Seo, S. Lee, Y. M. Kim and J. Kim, Lead optimization of a novel series of imidazo-[1, 2-a]-pyridine amides leading to a clinical candidate (Q203) as a multi-and extensively-drug-resistant anti-tuberculosis agent, *J. Med. Chem.*, 2014, 5293–5305.

13 Y. Cheng, G. C. Moraski, J. Cramer, M. J. Miller and J. S. Schorey, Bactericidal activity of an imidazo-[1, 2-a]-pyridine using a mouse *M. tuberculosis* infection model, *PLoS One*, 2014, **9**, 87483.

14 Z. Wu, Y. Lu, L. Li, R. Zhao, B. Wang, K. Lv and X. You, Identification of N-(2-phenoxyethyl)-imidazo-[1, 2-a]-pyridine-3-carboxamides as new antituberculosis agents, *ACS Med. Chem. Lett.*, 2016, **7**, 1130–1133.

15 G. Jose, S. Kumara, G. Nagendrappa, H. B. V. Sowmya, D. Sriram, P. Yogeeswari and L. V. Narendra, Synthesis, molecular docking and anti-mycobacterial evaluation of new imidazo-[1, 2-a]-pyridine-2-carboxamide derivatives, *Eur. J. Med. Chem.*, 2015, **89**, 616–627.

16 L. Pulipati, J. P. Sridevi, P. Yogeeswari, D. Sriram and S. Kantevari, Synthesis and anti-tubercular evaluation of novel dibenzo-[b, d]-thiophene tethered imidazo-[1, 2-a]- pyridine-3-carboxamides, *Bioorg. Med. Chem. Lett.*, 2016, **26**, 3135–3140.

17 H. Wang, A. Wang, J. Gu, L. Fu, K. Lv, C. Ma and Y. Lu, Synthesis and anti-tubercular evaluation of reduced lipophilic imidazo-[1, 2-a]-pyridine-3-carboxamide derivatives, *Eur. J. Med. Chem.*, 2019, **165**, 11–17.

18 A. Wang, K. Lv, L. Li, H. Liu, Z. Tao, B. Wang and Y. Lu, Design, synthesis and biological activity of N-(2-phenoxy)-ethyl-imidazo-[1, 2-a]-pyridine-3-carboxamides as new anti-tubercular agents, *Eur. J. Med. Chem.*, 2019, **178**, 715–725.

19 L. A. Li, B. Wang, M. Wang, K. Liu, Z. Tao Lv and Y. Lu, N-(2-Phenoxy)-ethyl-imidazo- [1, 2-a]-pyridine-3-carboxamides containing various amine moieties, Design, synthesis and anti-tubercular activity, *Chin. Chem. Lett.*, 2020, **31**, 409–412.

20 G. Samala, R. Nallangi, P. B. Devi, S. Saxena, R. Yadav, J. P. Sridevi and D. Sriram, Identification and development of 2-methylimidazo-[1, 2-a]-pyridine-3-carboxamides as *Mycobacterium tuberculosis* pantothenate synthetase inhibitors, *Bioorg. Med. Chem.*, 2014, **22**, 4223–4232.

21 A. Nandikolla, S. Srinivasarao, Y. M. Khetmalis, B. K. Kumar, S. Murugesan, G. Shetye and K. V. G. C. Sekhar, Design, synthesis and biological evaluation of novel 1, 2, 3-triazole analogues of Imidazo-[1, 2-a]-pyridine-3-carboxamide against *Mycobacterium tuberculosis*, *Toxicol. In Vitro*, 2021, **74**, 105137.

22 G. Samala, P. B. Devi, R. Nallangi, P. Yogeeswari and D. Sriram, Development of 3-phenyl-4, 5, 6, 7-tetrahydro-1H-pyrazolo-[4, 3-c]-pyridine derivatives as novel *Mycobacterium tuberculosis* pantothenate synthetase inhibitors, *Eur. J. Med. Chem.*, 2013, **69**, 356–364.

23 A. T. Manvar, R. R. Pissurlenkar, V. R. Virsodia, K. D. Upadhyay, D. R. Manvar, A. K. Mishra and E. C. Coutinho, Synthesis, in vitro anti-tubercular activity and 3D-QSAR study of 1, 4-dihydropyridines, *Mol. Diversity*, 2010, **14**, 285–305.

24 S. Konduri, J. Prashanth, V. S. Krishna, D. Sriram, J. N. Behera, D. Siegel and K. P. Rao, Design and synthesis of purine connected piperazine derivatives as novel inhibitors of *Mycobacterium tuberculosis*, *Bioorg. Med. Chem. Lett.*, 2020, **30**, 127512.

25 R. Narasimha, P. V. Rao, J. M. Saketi, N. V. Balaji, C. M. Kurmarayuni, G. V. Subbaraju and H. B. Bollikolla, Synthesis of new Hispolon derived pyrazole sulfonamides for possible antitubercular and antimicrobial agents, *J. Mex. Chem. Soc.*, 2021, **65**, 237–246.

26 G. Jose, T. S. Kumara, G. Nagendrappa, H. B. V. Sowmya, D. Sriram, P. Yogeeswari and L. V. Narendra, Synthesis, molecular docking and anti-mycobacterial evaluation of new imidazo [1, 2-a] pyridine-2-carboxamide derivatives, *Eur. J. Med. Chem.*, 2015, **89**, 616–627.

27 M. B. de Ávila, G. Bitencourt-Ferreira and W. F. de Azevedo, Structural basis for inhibition of enoyl-[acyl carrier protein] reductase (InhA) from *Mycobacterium tuberculosis*, *Curr. Med. Chem.*, 2020, **27**, 745–759.

28 M. Y. Lone, M. Athar, V. K. Gupta and P. C. Jha, Identification of *Mycobacterium tuberculosis* enoyl-acyl carrier protein reductase inhibitors: A combined *in-silico* and *in-vitro* analysis, *J. Mol. Graphics Modell.*, 2017, **76**, 172–180.

29 L. A. Collins and S. G. Franzblau, Microplate alamar blue assay versus BACTEC 460 system for high-throughput screening of compounds against *Mycobacterium tuberculosis* and *Mycobacterium avium*, *Antimicrob. Agents Chemother.*, 1997, **41**, 1004–1009.

30 S. G. Franzblau, R. S. Witzig, J. C. McLaughlin, P. Torres, G. Madico, A. Hernandez, M. T. Degnan, M. B. Cook, V. K. Quenzer, R. M. Ferguson and R. H. Gilman, Rapid, low-technology MIC determination with clinical *Mycobacterium tuberculosis* isolates by using the microplate Alamar Blue assay, *J. Clin. Microbiol.*, 1998, **36**, 362–366.

31 X. He, A. Alian, R. Stroud and P. R. Ortiz de Montellano, Pyrrolidine carboxamides as a novel class of inhibitors of enoyl acyl carrier protein reductase from *Mycobacterium tuberculosis*, *J. Med. Chem.*, 2006, **49**, 6308–6323.

32 S. K. Burley, H. M. Berman, C. Bhikadiy, C. Bi, L. Chen, L. Di Costanzo and C. Zardecki, RCSB Protein Data Bank: Biological macromolecular structures enabling research and education in fundamental biology, biomedicine, biotechnology and energy, *Nucleic Acids Res.*, 2019, **47**, D464–D474.

33 S. Pola, K. K. Banoth, M. Sankaranarayanan, R. Ummani and A. Garlapati, Design, synthesis, in silico studies and evaluation of novel chalcones and their pyrazoline derivatives for antibacterial and antitubercular activities, *Med. Chem. Res.*, 2020, **29**, 1819–1835.

